DEVELOPMENT OF SINGLE CHAIN POLYPEPTIDE-LOADED LIPOSOMES FOR OPHTHALMIC USE
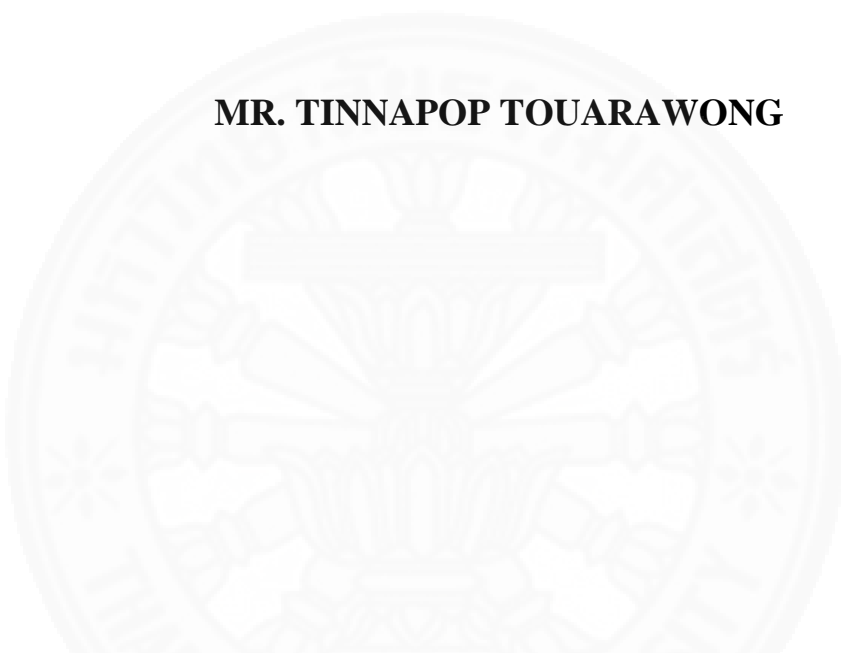
BY

MR. TINNAPOP TOUARAWONG

A THESIS SUBMITTED IN PARTIAL FULFILLMENT OF
THE REQUIREMENTS FOR THE DEGREE OF MASTER
OF SCIENCE (CHEMISTRY)
DEPARTMENT OF CHEMISTRY
FACULTY OF SCIENCE AND TECHNOLOGY
THAMMASAT UNIVERSITY
ACADEMIC YEAR 2016
COPYRIGHT OF THAMMASAT UNIVERSITY

DEVELOPMENT OF SINGLE CHAIN
POLYPEPTIDE-LOADED LIPOSOMES
FOR OPHTHALMIC USE

BY

MR. TINNAPOP TOUARAWONG

A THESIS SUBMITTED IN PARTIAL FULFILLMENT OF
THE REQUIREMENTS FOR THE DEGREE OF MASTER
OF SCIENCE (CHEMISTRY)
DEPARTMENT OF CHEMISTRY
FACULTY OF SCIENCE AND TECHNOLOGY
THAMMASAT UNIVERSITY
ACADEMIC YEAR 2016
COPYRIGHT OF THAMMASAT UNIVERSITY

THAMMASAT UNIVERSITY

FACULTY OF SCIENCE AND TECHNOLOGY
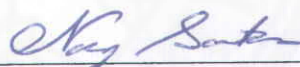
THESIS

BY

MR. TINNAPOP TOUARAWONG

ENTITLED

DEVELOPMENT OF SINGLE CHAIN POLYPEPTIDE-LOADED
LIPOSOMES FOR OPHTHALMIC USE

was approved as partial fulfillment of the requirements for
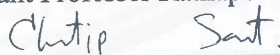the degree of Master of Science (Chemistry)

on May 1 , 2017

Chairman _____

(Professor Narong Sarisuta, Ph.D.)

Member and Advisor _____

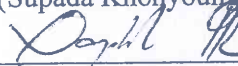(Assistant Professor Rathapon Asasutjarit, Ph.D.)

Member and Co-advisor _____

(Assistant Professor Chanatip Samart, Ph.D.)

Member _____

(Supada Khonyoung, Ph.D.)

Member _____

(Woraphol Rattanachuen, Ph.D.)

Dean _____

(Associate Professor Pakorn Sermsuk, M.Sc.)

Thesis Title	DEVELOPMENT OF SINGLE CHAIN POLYPEPTIDE-LOADED LIPOSOMES FOR OPHTHALMIC USE
Author	Mr. Tinnapop Touarawong
Degree	Master of Science (Chemistry)
Major Field/Faculty/University	Department of Chemistry Faculty of Science and Technology Thammasat University
Thesis Advisor	Assistant Professor Rathapon Asasutjarit, Ph.D.
Thesis Co-Advisor	Assistant Professor Chanatip Samart, Ph.D.
Academic Years	2016

ABSTRACT

Corneal abrasion is a one of serious ocular injuries. Its clinical problem not only causes eye irritation but also leads to visual loss. Generally, several therapeutic agents have been used as a supportive medication treatment which is unable to enhance healing process. Currently, single chain polypeptides (SCP) have been used as a wound healing enhancer in ocular injury. SCP could promote cell proliferation in wound healing process of injured ocular tissue. However, a restriction for SCP ophthalmic delivery is poor bioavailability because of its high molecular weight and anatomical and physiological constraints of the eyes. Recently, liposomes have been introduced to improve bioavailability of macromolecule drugs such as protein in ophthalmic delivery. However, the limitation factor of liposomal products was physicochemical instability. Thus, this study intended to prepare lyophilized SCP-loaded liposomes (LSCP-LPs) for SCP ophthalmic delivery and to investigate their physical stability. SCP-loaded liposomes (SCP-LPs) were prepared by reverse-phase evaporation technique (REV). SCP was loaded to liposomes by ultrasonic force and then made SCP-LPs dry by lyophilization technique.

SCP-LPs and LSCP-LPs were evaluated their physicochemical properties, physical stability, *in vitro* drug release, and pharmacological activities. It was found that LSCP-LPs had spherical shape with diameter of 81.56±0.13 nm. Their polydispersity index (PDI) was 0.23±0.00, zeta potential: -2.90±0.03 mV, and drug entrapment efficiency: 73.28±0.93%. They had X-ray powder diffraction analysis of LSCP-LPs revealed that the molecules of composition of LSCP-LPs were arranged and transformed to amorphous organization. Investigation of fourier transform-infrared spectroscopy technique indicated that SCP could embed in lipid bilayer of LSCP-LPs. The results of stability test revealed that particle size, PDI, zeta potential, and drug entrapment efficiency of LSCP-LPs under storage temperature of 4°C were not significantly different from the initial day. The *in vitro* drug release study of LSCP-LPs showed that SCP release profile of LSCP-LPs was best fitted with Higuchi's model. The results of *in vitro* eye irritation test and *in vitro* cell proliferation-promoting activity test of LSCP-LPs in SIRC cells exhibited that LSCP-LPs did not show irritation effects, but they had higher potential for promoting cell proliferation of SIRC cells compared to empty liposomes (LPs). Consequently, LSCP-LPs had potential for use in further *in vivo* study for corneal abrasion treatment.

ACKNOWLEDGEMENTS

TABLE OF CONTENTS

LIST OF TABLES

LIST OF FIGURES

LIST OF ABBREVIATIONS

Symbols/Abbreviations	Terms
%	Percent
$\times g$	Times gravity
°	Degree
°C	Degrees Celsius
μ	Micro
Å	Angstrom
ANOVA	Analysis of variance
ATR	Attenuated total reflection
C=O	Carbonyl group
C18	Carbon chain18
-CH	Hydrocarbon group
cm	Centimeter
CMC	Critical micelle concentration
Cont.	Continue
CuK_{α}	Copper K-alpha
CV	Cell viability
df	Degrees of freedom
DSC	Differential scanning calorimetry
EGFR	Epidermal growth factor receptor
EMEM	Eagle's minimum essential medium etrazolium bromide) tetrazolium reduction assay
FT-IR	Fourier transform-infrared spectroscopy
g	Gram
GPC	Gel-permeation chromatography

GUV	Giant unilamellar vesicle
HES	Hydroxyethyl starch
hrs	Hours
J	Joule
JAK	Intracytoplasmic janus kinase
kDa	Kilodalton
kHz	Kilohertz
LC	Liquid chromatography-column
LPs	Liposomes
LSCP-LPs	Lyophilized single chain polypeptide-loaded liposomes
LUV	Large unilamellar vesicle
mAU	Milli-absorbance unit
Min	Minute
mL	Milliliter
MLV	Multilamellar vesicle
mm	Millimeter
mPa	Millipascal
MTT	3-(4,5-dimethylthiazol-2-yl)-2,5-diphenyltetrazolium bromide
mV	Millivolt
MVV	Multivesicular vesicle
nm	Nanometer
NSAIDs	Nonsteroidal anti-inflammatory drugs
-OH	Hydroxyl group
OLV	Oligolamellar vesicle
PBS	Phosphate buffer saline solution
PCS	Photon correlation spectroscopy technique
PDI	Polydispersity index

PEG	Polyethylene glycol
pI	Isoelectric point
PVP-10	Polyvinylpyrrolidone-10
PVP-40	Polyvinylpyrrolidone-40
R^2	Coefficient of determination
REV	Reverse-phase evaporation technique
RPE	Retinal pigment epithelium
RP-HPLC	Reverse phase-high performance liquid chromatography technique
RSCP-LPs	Reconstituted single chain polypeptide-loaded liposomes
SCP	Single chain polypeptides
SCP-LPs	Single chain polypeptide-loaded liposomes
SD	Standard deviation
sec	Second
SIRC	Statens seruminstitut rabbit corneal cells
STAT	Signal transducer-activator of transcription
STE	Short time exposure test
SUV	Small unilamellar vesicle
T_{front}	Sublimation front temperature
T_g	Glass transition temperature
T_g'	Glass transition temperature of maximally freeze-concentrated fraction
T_m	Melting temperature
UV	Ultraviolet detector
W_o	Initial weight of drug content
W_t	Weight of drug content
XRD	X-ray powder diffraction analysis
α	Alpha

CHAPTER 1

INTRODUCTION

The general case of ocular injuries is corneal abrasion (scratched cornea) which is usually found in ocular trauma, contact lenses, corneal dystrophy, epidemic kera-toconjunctivitis, and post-operative conditions. It not only causes eye irritation but also leads to visual loss. Although, there are numerous therapeutic agents for relieving symptoms of corneal abrasion available in drug markets such as topical analgesics, topical antibiotics, and oral analgesics (Wipperman et al., 2013) but their therapeutic agents are just supportive treatments without wound healing activity. Recently, SCP is an essential therapeutic agent for promoting cell proliferation, cell migration, and re-epithelialization for wound healing process in various tissues. It has been introduced for using in ocular injuries (Sacchetti et al., 2014). Moreover, SCP has been utilized in several pharmacological conditions such as treatment of various wounds, targeted therapeutic agents for against cancers (Lurje et al., 2009), and support collagen production in many tissues (Throm et al., 2010). However, the important restrictions for ophthalmic delivery especially macromolecules like SCP are anatomical and physiological conditions of the eyes such as tear turnover, nasolacrimal drainage, and ocular tissue barriers leading to poor ocular bioavailability (Gaudana et al., 2010).

In previous studies, the liposomal technology has been used for ophthalmic drug delivery system in various ocular diseases such as glaucoma, ocular infection, and ocular inflammation (Hathout et al., 2007; Abdelbary et al., 2011; Fujisawa et al., 2012). Moreover, many studies demonstrated that liposomes had advantages for ocular drugs delivery such as high corneal penetration, high biocompatibility, and non-cytotoxic (Ashaben et al., 2013) leading to increment of bioavailability of the delivered drugs. Until now, it still lacks data of using liposomes as an ophthalmic drug delivery system for SCP.

A major disadvantage of liposomes for drug delivery is physicochemical instability via several chemical reactions such as oxidation, hydrolysis, especially at high temperature environments (Himanshu et al., 2011; Kataria et al., 2011).

The most common chemical instability of liposomes is induced by hydrolysis reaction because a hydrophilic part of phospholipid consisting of liposomes is a target for being attacked by nucleophiles. This reaction causes aggregation and leakage of liposome vesicles (Ghanbarzadeh et al., 2013).

Nowadays, a strategy for increasing physicochemical stability of liposomal products and sensitive therapeutic agents is lyophilization which is a technique performed under a low-pressure condition to remove water molecules from frozen liposomal products. Even though, lyophilization technique is a high potential technique for increasing long-term stability of liposomal products, it can generate unsuitable conditions during solidification (freezing phase) and drying process leading to degradation of lyophilized liposomal products such as vesicle aggregation, drug leakage, and liposomal structure degradation. Therefore, this study intended to develop production process of LSCP-LPs for ophthalmic use. The purposes of this research were:

1. To determine the effect of production process on physicochemical properties of LSCP-LPs.

2. To investigate chemical interaction of composition of LSCP-LPs.

3. To evaluate physical stability of LSCP-LPs.

4. To study *in vitro* drug release profile of LSCP-LPs.

5. To determine potential for being an eye irritant of LSCP-LPs.

6. To evaluate cell proliferation-promoting activity of LSCP-LPs.

CHAPTER 2
REVIEW OF LITERATURE

2.1 Ophthalmic Drug Delivery System

The topical ophthalmic medications in drug markets are the most common used in numerous ocular diseases such as glaucoma, allergic conjunctivitis, ocular infection, ocular lymphoma, corneal abrasion (scratched cornea), and post-operative conditions (Hathout et al., 2007; Abdelbary et al., 2011; Fujisawa et al., 2012). However, the major challenge of topical ophthalmic medications is poor bioavailability because anatomical and physiological conditions of ocular system such as tear turnover, nasolacrimal drainage, and ocular tissue barriers. Their conditions can be reduced drug concentration and resist deeply drug permeability in ocular tissues (Gaudana et al., 2010). Figure 2.1 is presented the various ophthalmic drug delivery systems to increase bioavailability of the delivered drugs i.e. nanomicelles, liposomes, dendrimers, nanospheres, and nanocapsules (Ashaben et al., 2013). Nowadays, liposomes is one of strategies to develop as the ophthalmic drug delivery system with many advantages such as high biocompatibility, high transcorneal permeation, and non-cytotoxicity.
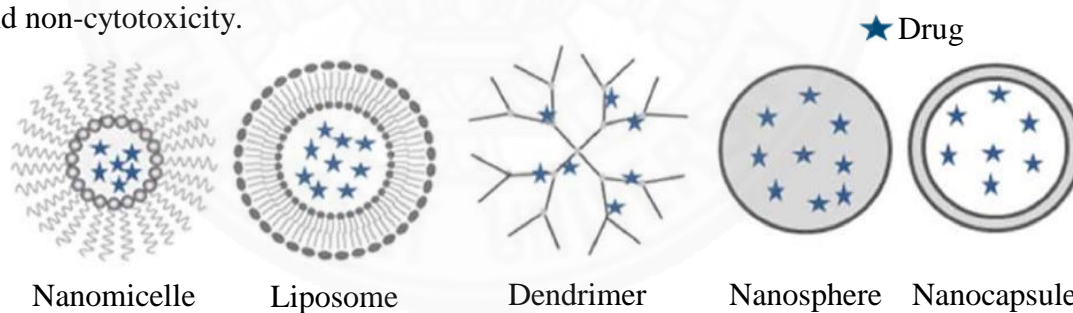
Figure 2.1 Nanocarriers for ophthalmic drug delivery.

2.2 Anatomical and Physiological of Ocular System

The ocular system is an essential organ of function of vision. The eyes are special organ with highly complicated anatomical and physiological conditions.

The ocular system can be classified into two major segments are anterior segment and posterior segment (Figure 2.2). The anterior segment of an ocular system has approximately one of third ocular system which the remaining ocular system has occupied by the posterior segment. The anterior segment of an ocular system is included (1) Limbus: the tissue layers between the sclera and the cornea. (2) Cornea: the outer transparency part of the anterior chamber. Cornea can be adjusted the lights for focus on the retina. Cornea layers are included. (2.1) Epithelium: the surface tissue layer of cornea which cover by tear film for protect the eyes from environmental. (2.2) Stroma: the supporting tissue layer of cornea and including keratocytes and collagen fibers. (2.3) Descemet's membrane: the inner tissue layer of cornea which their tissue is supported the function of endothelial cells. (2.4) Endothelium: this is an essential tissue layer of cornea which their tissue is comprising from collagen fibers. Their tissue can be protected and supported the cornea. (3) Conjuncttiva: this is a transparency mucous membrane. Their tissue will be covered the eye surface and protected the inner of ocular tissues. In addition, the inflammation of conjunctiva can be generated pink eyes which called conjunctivitis. (4) Iris: this is the colored area of the center of the eyes which appeared the cavity of the eye center called "pupil". The iris will be regulated pupil by iris muscle to modulate a light through in the eyes. (5) Ciliary body: this is an outer field area which attach the iris and near the eye wall. Ciliary body can be produced the essential fluids (aqueous humor) to maintain the structure of the eyes. Moreover, ciliary body will be supported structure transformation of the eye lens for focusing process of vision. (6) Aqueous humor: this is a chamber or space of the anterior of the eyes that consisting essential fluids to protect the eye structure. (7) Lens: this is a transparency part which immobilized by using small fibers (zonules) from the eye wall. Lens are located at anterior segment which behind iris and pupil of the eyes. Lens can be accommodated a light through into the eyes and supported the focusing process of the eyes by arrange their structure for vision process.

The posterior segment of the ocular system is included (1) Sclera: this is the white area of outer surface of the eye wall which cover on the major parts of the eyeballs.

The sclera is comprised from collagen fibers with vigorous layer of eyeball and consisted six extraocular muscles to maintain their structure. (2) Retinal pigment epithelium (RPE): this is an essential filed which located at deep cell layer of retina. This cell layer can be supported photoreceptor cells to maintain the function of the retina. (3) Vitreous humor: vitreous chamber is located at posterior segment which between the lens and the retina of the eyes. This chamber will be contained the essential fluid to maintain the inner eye structure. (4) Retina: this is a thin transparency layer which cover the inner of the eye wall. This layer will be consisted various cells in the inner eyes i.e. rod cells and cone cells (as a photoreceptor cells). The retina is the first imaging point and then transmitting the signal via optic nerve to the brain for eye vision process. (5) Choroid: this is a thin layer which locate at between the sclera and the retina. Choroid has numerous invasion of blood vessels for nourishment for the retina. (6) Optic nerve: this is an essential part for eye vision process by synchronize between of the eyes and the brain.
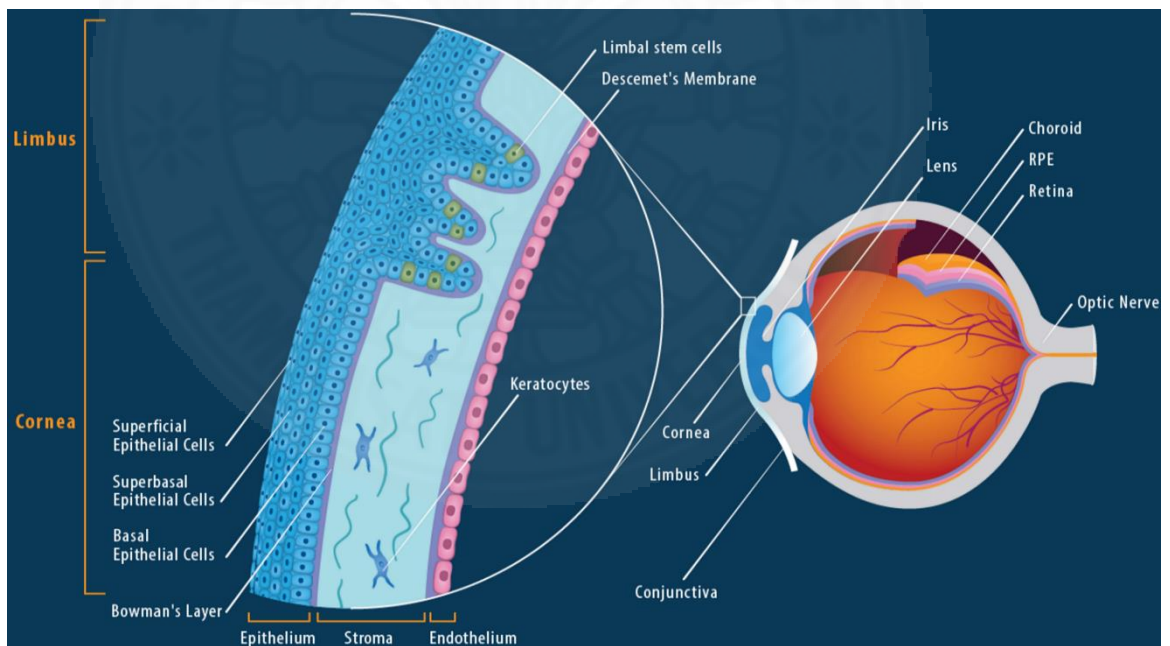
Figure 2.2 Anatomy of the ocular system and cornea.

2.3 Evaluation and Administration of Corneal Abrasion

The corneal abrasion (scratched cornea) is the one of serious ocular injuries and found that in ocular trauma, contact lenses, corneal dystrophy, ocular infection, allergic conjunctivitis, glaucoma, and post-operative conditions. The incident rate of corneal abrasion is eight percent of ocular disease in primary care unit. Generally, the most common case of corneal abrasion is accident situation and appeared severe ocular problem leading to loss quality of patient life. Moreover, the corneal abrasion can be induced irregular eye shape leading to loss of vision.

The diagnosis of corneal abrasion is evaluated severity level by physical eye examination to detect ocular infection, ocular trauma, and vision loss level. However, the important problem in injured ocular case is foreign matters. The penlight examination is performed to removal of foreign matters in ocular injuries case. In addition, the diagnosis of corneal abrasion is commonly used fluorescein eye staining. Briefly, fluorescein dye solution will be dropped on the injured cornea of the eyes and then evaluate the corneal defects. Figure 2.3 in **(a)** presented the yellow color on the injured corneal when diagnosis under normal lights. On the other hand, the green color will be appeared on corneal defect when diagnosis under ophthalmoscope with cobalt blue lights (Figure 2.3 in **(b)**).
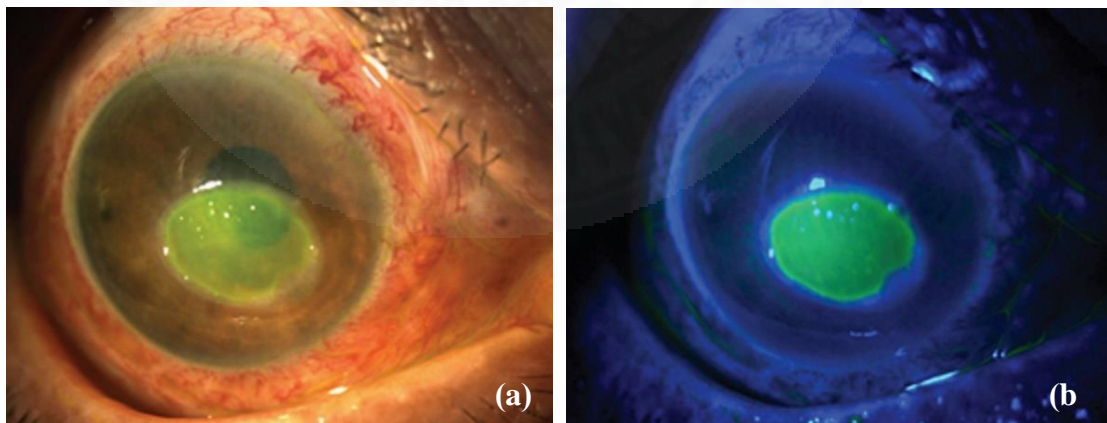
Figure 2.3 Corneal defects: **(a)** viewed in normal lights and **(b)** viewed in cobalt blue lights of ophthalmoscope.

Generally, the treatment goals of corneal abrasion are prevention of ocular infection, reduction of ocular inflammation, and rapid healing of injured cornea. Currently, various topical ophthalmic formulations available in drug markets for treatment of corneal abrasion are topical antibiotics, topical cyclopegics, and topical NSAIDs (Table 2.1). However, numerous therapeutic agents are just supportive medications which unable to enhance healing injured ocular tissues. Nowadays, single chain polypeptide (SCP) has been recently used in injured ocular tissue via mitogenic effects leading to recovery of their tissue.

Table 2.1 Topical ophthalmic medication for treatment of corneal abrasion.

Medications	Administration	Evidence level
1. Topical antibiotics		C
- 0.5% Erythromycin ointment	0.5-inch ribbon, four times per day for three to five days	
- Polymyxin B/trimethoprim Solution	1 drop, four times per day for three to five days	
- 10% Sulfacetamide solution	1 to 2 drops, four times per day for three to five days	
- 0.3% Ciprofloxacin ointment and solution	0.5-inch ribbon or 1 to 2 drops, four times per day for three to five days	
- 0.3% Gentamicin ointment and solution	0.5-inch ribbon or 1 to 2 drops, four times per day for three to five days	
- 0.3% Ofloxacin solution	1 to 2 drops, four times per day for three to five days	
2. Topical cycloplegics	1 drop, may repeat in five minutes if	B
- 1% Cyclopentolate solution	needed	
	1 drop, may repeat in five minutes if	
- 5% Homatropine	needed	

Table 2.1 Topical ophthalmic medication for treatment of corneal abrasion (Cont.).

Medications	Administration	Evidence level
3. Topical NSAIDs	1 drop, four times per day for two to	B
- 0.1% Diclofenac solution	three days	
	1 drop, four times per day for two to	
- 0.4% Ketorolac solution	three days	

2.4 Application of SCP

Over past of decade, numerous growth factors are utilized to healing injured tissues. Growth factors have been used mitogenic effects to promoting cell proliferation, cell differentiation, and cell migration (Menke et al., 2007). The first succession of SCP isolation (SCP was extracted form submaxillary gland of the mouse) by Stanley Cohen in 1962. SCP has been utilized as a wound healing enhancer with high potential therapeutic agents in various cells i.e. epidermal cells, endothelial cells, fibroblast cells, glial cells, and corneal endothelial cells. Generally, SCP is a small mitogenic polypeptide (Figure 2.4) and comprising from 53 amino acids (chemical properties of SCP: molecular weight 6045 kDa, pI 4.6, and three intramolecular disulfide bonds).

Figure 2.4 Chemical structure of SCP.

Basically, action mechanism of SCP (Figure 2.5) explained by Konkimalla et al. (2009). Briefly, SCP will be interacted extracellular domain of SCP receptor (signal transducer-activator of transcription: STAT) with high affinity interactions. After that, SCP can be generated dimerization of ligands of SCP receptors. The cytoplasmic membrane of SCP receptor (intracytoplasmic janus kinase: JAK) will be induced transphosphorylation to tyrosine residues in the cytoplasmic domain of SCP receptor. The phosphorylated tyrosine of SCP receptor will be stimulated intracellular proteins called GRB2 and SOS. Then, their proteins can be induced increment of glycolysis and protein synthesis of cells and then stimulate gene transcription leading to cell proliferation, inhibition of apoptosis, re-epithelialization, and cell migration.

Nowadays, SCP has been used in many clinical cases with high safety and efficiency in treatment of gastric ulcers (Tanigawa et al., 2015; Celebi et al., 2002; Li et al., 2003), injured cornea (Klenkler et al., 2007; Wang et al., 2009), diabetic ulcers (Mohan et al., 2007; Martínez et al., 2013), and wound healing (Degim et al., 2007; Gil et al., 2013; Barrientos et al., 2014).
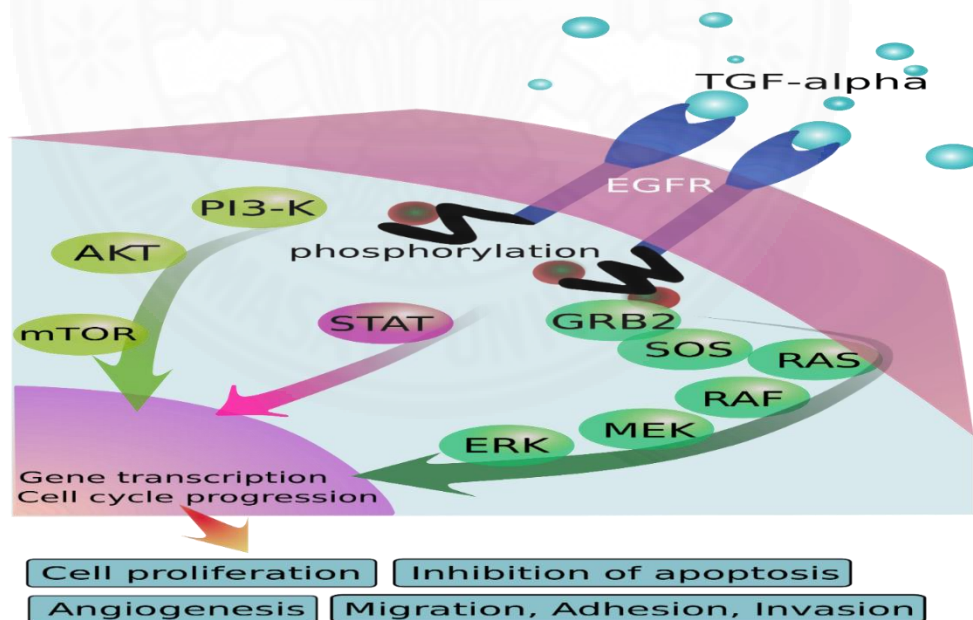
Figure 2.5 Mechanism of action of SCP.

2.5 Liposomes

Liposomes is comprised from organization of phospholipid molecules by using Van der Waals interaction. Figure 2.6 demonstrated the phospholipid molecules in liposomal structure which included hydrophilic part and hydrophobic part. The hydrophilic part of phospholipid molecule included 3 major parts are polar head group (such as ethanol-mine, choline, and serine), phosphate group, and glycerol. In addition, the hydrophobic part of phospholipid molecule is comprised from saturated fatty acid chain i.e. arachidic acid, steric acid, and palmitic acid and/or unsaturated fatty acid chain i.e. erucic acid, oleic acid, linoleic acid, and linolenic acid.
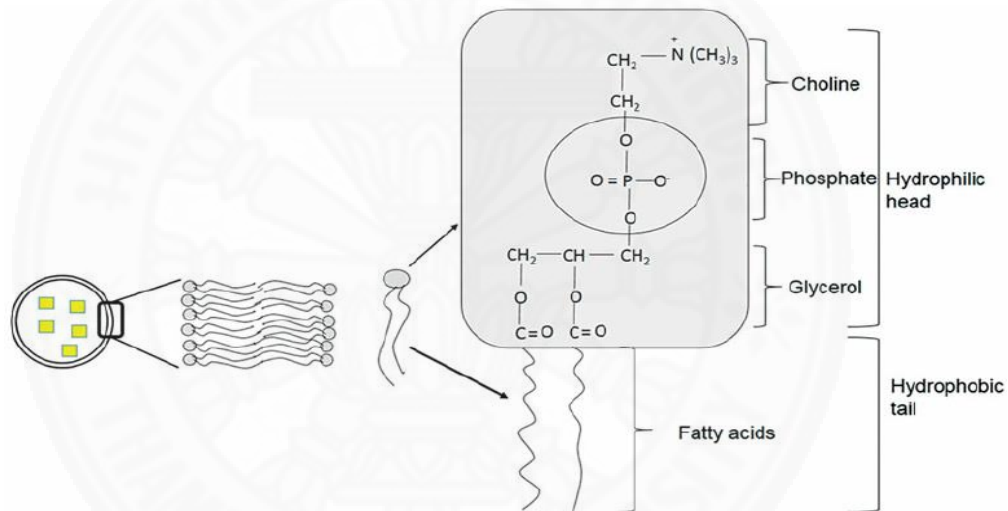
Figure 2.6 Chemical structure of phospholipid molecule in liposomes.

2.5.1 Classification of Liposomes

Generally, liposomes can be classified by using particle diameter (usually found in a range of 20 nm to 200 µm) and type of lamellar vesicle. In addition, the form of lamellar vesicle of liposomes is consisted one or more phospholipid bilayers. Figure 2.7 presented the classification of liposomes are small unilamellar vesicle (SUV), large unila-mellar vesicle (LUV), giant unilamellar vesicle (GUV), oligolamellar vesicle (OLV), multi lamellar vesicle (MLV), and multivesicular vesicle (MVV).
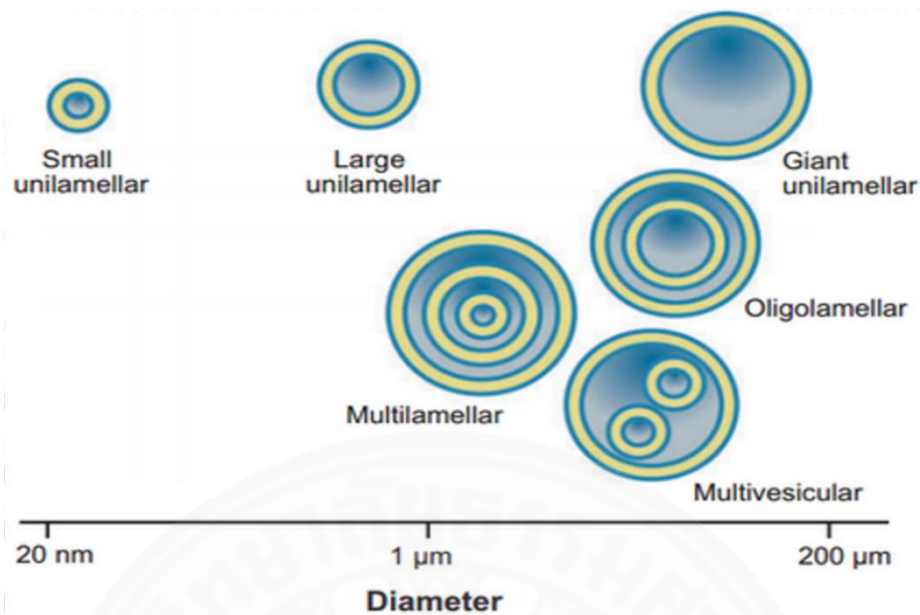
Figure 2.7 Classification of liposomes.

2.5.2 Method of Liposomes Preparation

Currently, method of liposomes preparation can be classified into 3 major techniques as the follows in Table 2.2 (Shashi et al., 2012).

Table 2.2 Method of liposomes preparation.

Preparation method	Type of liposomal vesicle
1. Mechanical dispersion method	
- Thin-film hydration method	MLV
- Sonication method	SUV
- French pressure cell method	SUV
2. Solvent dispersion method	
- Ethanol injection method	MLV, OLV, and LUV
- Ether injection method	MLV, OLV, and SUV
- Reverse-phase evaporation method	MLV, OLV, and SUV
3. Detergent removal method	MLV, OLV, and LUV

2.5.2.1 Mechanical Dispersion Method

(1) Thin-Film Hydration Method

This is a conventional method and most widely used because this technique is uncomplicated method for preparation of various liposomal products (Figure 2.8). Briefly, phospholipid and cholesterol are dissolved in organic solvent. The lipid mixture solution will be eliminated organic solvent by rotary evaporator under low pressure condition to obtain lipid dried film. After that, nitrogen gas (other inert gases) will be flushed into their film to removal of organic solvent residues and generate complete swelling film form. Then, aqueous part will be introduced into lipid dried film and performed under high temperature at above glass transition temperature (T_g) of phospholipid to obtain liposomal dispersion. This is due to the fact that the high temperature above glass transition temperature can be increased flexibility and permeability of lipid bilayer in liposomes leading to increment of drug encapsulation efficiency in liposomes.
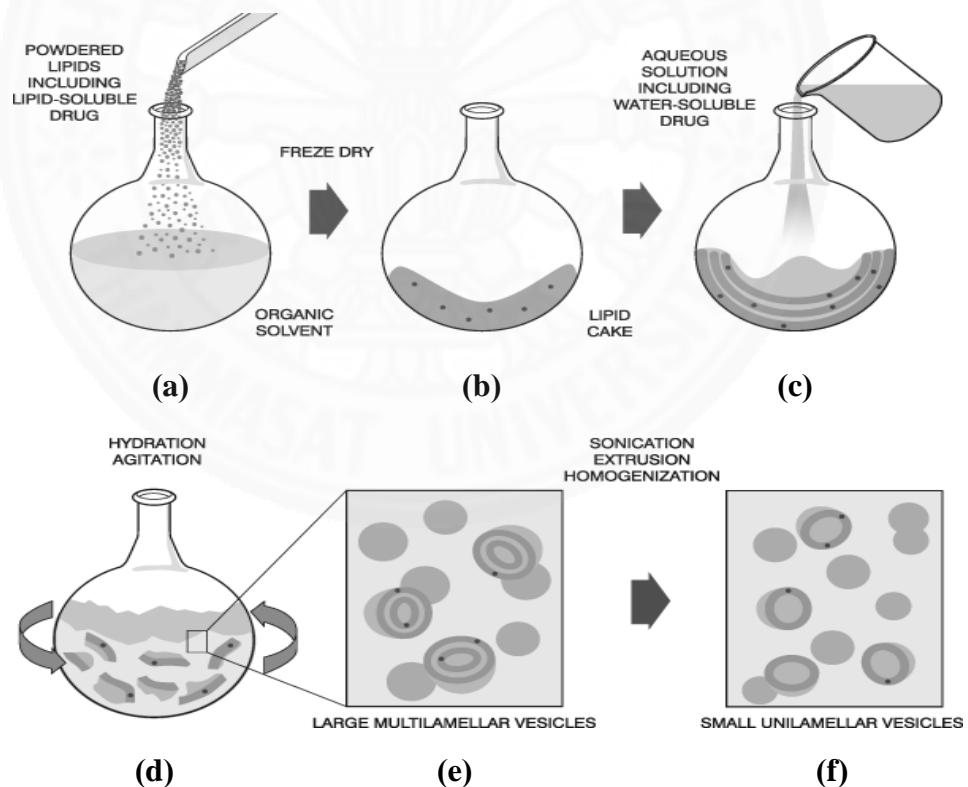
Figure 2.8 Thin-film hydration method of liposomes preparation.

(2) Sonication Method

Although, thin-film hydration method is widespread used to prepare liposomal products but obtained liposomes is appeared large particle diameter. Therefore, sonication technique is one of preparation techniques to improve particle size of liposomes. This is due to the fact that energy supplied of ultrasonic waves (mechanic forces) can be stimulated phospholipid molecules of lipid bilayer of liposomes. Therefore, the particles of liposomes are broken down into smaller liposomes (Akbarzadeh et al., 2013). Generally, the sonication technique can be classified into 2 groups are bath sonicator and probe sonicator (Figure 2.9). (1) Bath sonicator: liposomes are transferred into cylindrical glass container and then applied into bath sonicator which conducted under high temperature above T_g of phospholipid to obtain suitable particle diameter of liposomes. (2) Probe sonicator: this technique is directly applied energy input of ultrasonic waves into liposomes. In addition, this technique is used lower sonication time consumption compared to bath sonicator. However, this technique can be generated many unsuitable conditions to liposomes i.e. contamination of heavy metal (titanium), lower drug entrapment efficiency, and liposomal degradation.
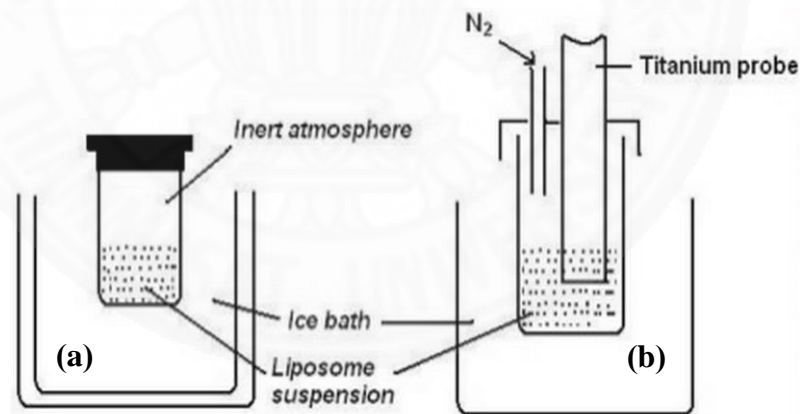
Figure 2.9 Sonication method of liposomes preparation: **(a)** bath sonicator and **(b)** probe sonicator.

(3) French Pressure Cell Method

Generally, this technique is widely used in sensitive materials with several advantages than sonication method such as non-contamination of heavy metal, suitable in thermolabile materials, large production scale, and appropriate particle diameter. Briefly, liposomes will be extruded by using small orifice called "piston" with controllable pressure condition to obtain appropriate particle diameter of liposomes (Figure 2.10).
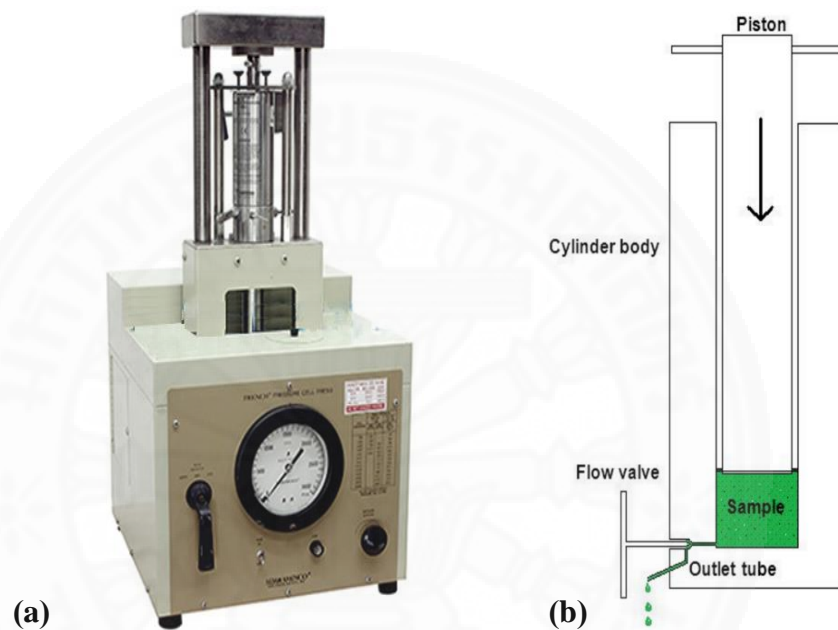
Figure 2.10 French pressure cell method of liposomes preparation: **(a)** French pressure cell machine and **(b)** component diagram of French pressure cell.

2.5.2.2 Solvent Dispersion Method

(1) Solvent Vaporization Method

- Ethanol injection method: this technique is most commonly used to obtain small particle diameter of liposomes. Briefly, lipid mixture in ethanol solution will be rapidly injected into aqueous chamber with high temperature to eliminate ethanol residues and obtain small particle diameter of liposomes (Figure 2.11 in **(a)**).

However, this technique can be generated many stresses i.e. contamination of ethanol residues, non-thermolabile materials, and liposomal degradation.

- Ether injection method: this technique is widespread used to obtain appropriate particle diameter of liposomes. Briefly, lipid mixture in ether solution is injected into aqueous chamber with high temperature to eliminate ether residues and obtain smaller particle diameter of liposomes (Figure 2.11 in **(b)**). However, this technique will be generated several unsuitable conditions i.e. unsuitable in sensitive materials, degradation of liposomes, and contamination of ether residues.

(a)

(b)
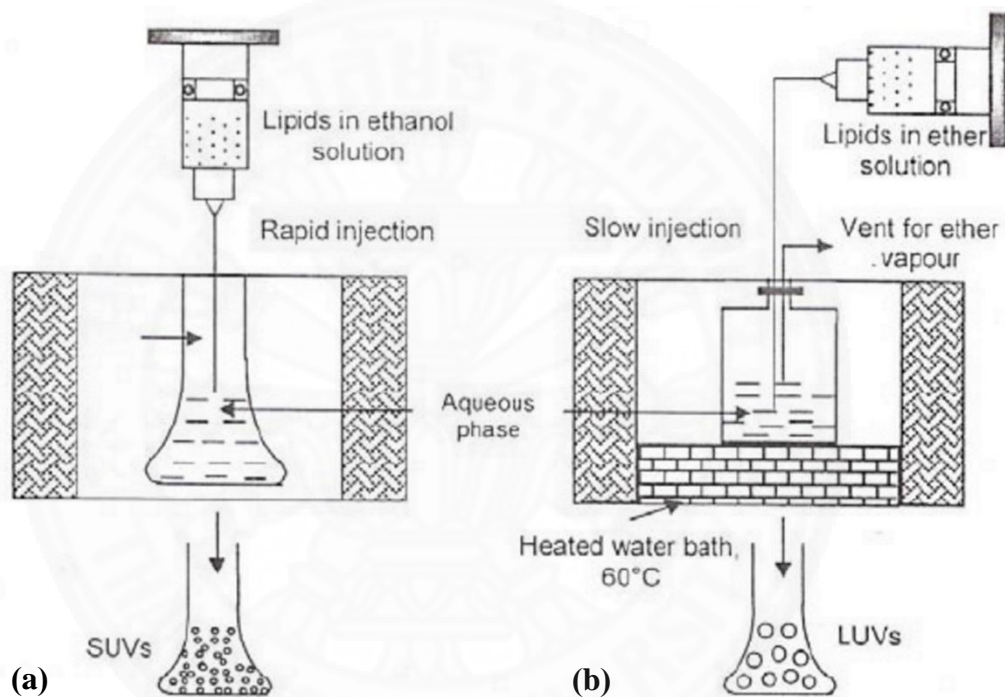
Figure 2.11 Solvent vaporization method of liposomes preparation: **(a)** ethanol injection method and **(b)** ether injection method.

(2) Reverse-Phase Evaporation Method (REV)

This technique is the most commonly used in various liposomal formulations. Because of this technique is a simple method to prepare liposomal products with highly drug entrapment efficiency. In addition, this technique can be encapsulated various therapeutic agents (Himanshu et al., 2011; Kataria et al., 2011).

Briefly, phospholipid and cholesterol are dissolved in organic solvent. The lipid mixture solution will be introduced into aqueous part and then immediately sonicated to obtain water-in-oil emulsions (inverted micelles). After that, their mixture will be eliminated organic solvent by using rotary evaporator which conducted under low heating temperature and reduced pressure condition for conversion of inverted micelles into liposomes. The excess of phospholipid molecules in the system will be donated to the formation of lipid bilayer of liposomes. Finally, liposomes were obtained (Figure 2.12).
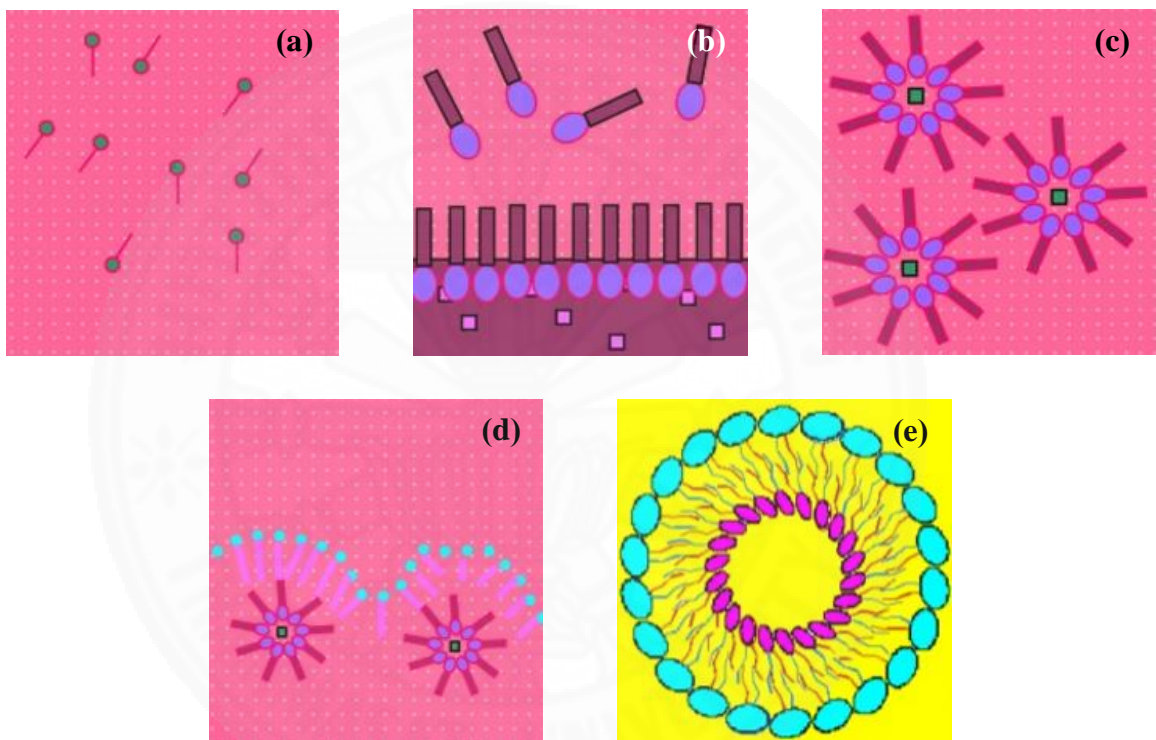
Figure 2.12 Formation mechanism of Liposomes in REV method.

2.5.2.3 Detergent Removal Method

This technique is a widespread used in numerous liposomal products which uncomplicated method and gentle condition for various sensitive materials. Briefly, phospholipid, cholesterol, drugs, and detergent (i.e. cholate, alkyl glycoside, and Triton X-100) are dissolved in aqueous phase at critical micelle concentration (CMC).

After that, liposomes will be transferred into dialysis bag to remove detergents leading to formation of liposomes (Figure 2.13). In addition, elimination of detergent residues can be utilized detergent adsorbent (polystyrene-divinyl-benzene beads) and gel permeation chromatography technique (GPC). However, this technique has several disadvantages i.e. incompatibility, material degradation (hydrolysis reaction), contamination of detergent residues, and high production time consumption.
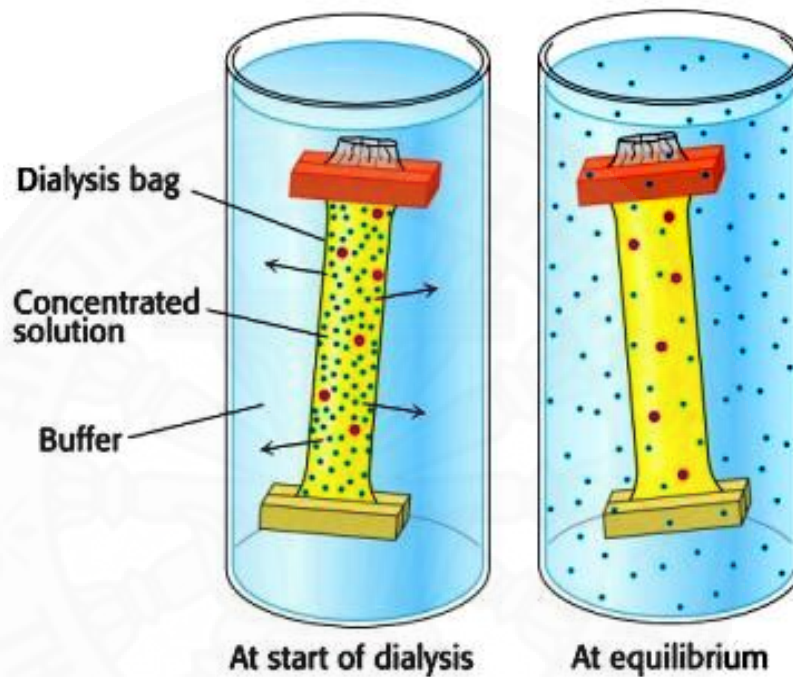
Figure 2.13 Dialysis technique of detergent removal method of liposomes preparation.

2.5.3 Lyophilization Technique of Liposomal Product

Lyophilization technique (freeze-drying technique) is an essential technique to eliminate aqueous part from frozen products which performed under extremely low pressure condition leading to long-term storage of products. Moreover, this technique is utilized in various sensitive therapeutic agents including proteins, vaccines, gene, and liposomal products. Currently, liposomal products can be destabilized their physicochemical stability by aqueous part in their products.

This is due to the fact that nucleophiles of aqueous part in the liposomal products can be attacked lipid bilayer of liposomes by hydrolysis reaction. In addition, water molecules will be interacted ester group in glycerol part of phospholipid molecule leading to liposomal degradation such as vesicle aggregation, drug leakage, and reduction of zeta potential. Over the past decade, several studies were reported lyophilized liposomal products had higher physicochemical properties (i.e. particle diameter, PDI, and drug entrapment efficiency) compared to liquid liposomal formulations.

Although, this technique is the high potential technique for increment of long term stability in liposomal products. However, this technique can be generated many stresses when using unsuitable condition of lyophilization process and cryoprotectant concentration leading to destabilization of liposomal products.

Generally, lyophilization technique can be classified into 3 major processes (Kasper et al., 2011) included (1) freezing phase (solidification), (2) primary drying phase (ice sublimation), and (3) secondary drying phase (desorption of residue water).

2.5.3.1 Freezing Phase (Solidification)

The freezing phase is one of the essential process in lyophilization. This process will be applied super-cooling into liposomal products leading to frozen state in ice crystal formation. However, this process can be generated several stresses from dendritic ice crystals leading to liposomal degradation. Therefore, appropriate freezing temperature is a necessary factor to increase physicochemical stability of lyophilized liposomes.

However, cryoprotectants is an essential factor to protect and maintain liposomal structure leading to reduction of physicochemical instability in lyophilized liposomal products i.e. sucrose, trehalose, and mannitol (Ola et al., 2010). Figure 2.14 demonstrated cryoprotectants can be formed hydrogen bond and replaced water molecules of hydrophilic head of phospholipids in liposomes. In addition, unsubstituted cryoprotectants will be generated glassy matrix (amorphous organization) surround and protect particle of liposomes during lyophilization (Chen et al., 2010).

(a)   **(b)**   **(c)**

(d)   **(e)**   **(f)**
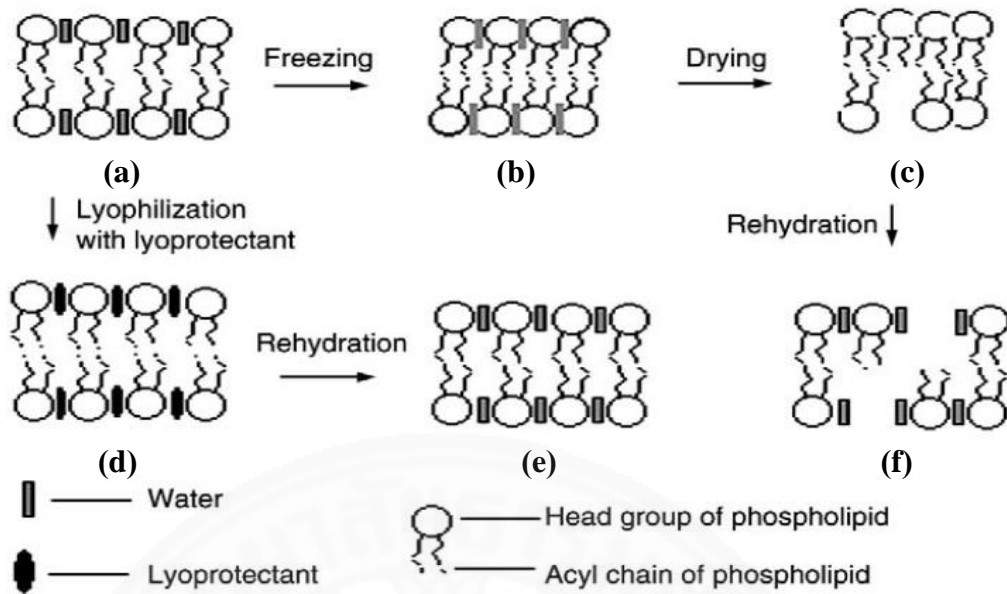
Figure 2.14 Mechanism of cryoprotectants and liposomes during lyophilization.

Nevertheless, glass transition temperature of maximally freeze-concentrated fraction (T_g') of cryoprotectants are the essential factors in lyophilization. This factor can be explained by using binary systems of water and sucrose. Sucrose solution in solidification will be increased their concentration when reach T_g' during solidification. Sucrose in this temperature had not change their concentration and high potential to cover particle of liposomes leading to protection of their structure. Therefore, freezing temperature during solidification should be below T_g' of cryoprotectants to maintain protection potential of cryoprotectant leading to increment of physicochemical stability of lyophilized products (Table 2.3).

Table 2.3 T_g' of cryoprotectant for lyophilization.

Cryoprotectants	T_g' (°C)
1. Sugars	
- Xylose	-48.0
- Ribose	-47.0
- Glucose	-43.0
- Fructose	-42.0
- Galactose	-41.5
- Mannose	-41.0
- Sucrose	-32.0
- Maltose	-29.5
- Trehalose	-29.5
- Lactose	-28.0
2. Polyalcohols	
- Ethylene glycol	-85.0
- 1,3-butanediol	-63.5
- Glycerol	-65.0
3. Polymers	
- Polyethylene glycol (PEG)	-63.5
- Polyvinylpyrrolidone-10 (PVP-10)	-26.0
- Polyvinylpyrrolidone-40 (PVP-40)	-20.5
- Gelatin	-8.0
- Dextran	-13.5
- Hydroxyethyl starch (HES)	-6.5

2.5.3.2 Primary Drying Phase (Ice sublimation)

Primary drying phase is sublimation of ice crystal formation in matrix of frozen liposomal products (porous cake) which perform after solidification. Temperature of sublimation front (T_{front}) is a necessary factor in primary drying phase. In primary drying phase, T_{front} should be below T_g' of cryoprotectant. This is due to the fact that high T_{front} can be reduced surface area of matrix in porous cake and generated incomplete dried lyophilized liposomes leading to destabilization of physicochemical stability of their products. Nevertheless, primary drying phase cannot complete eliminated water residues in dried lyophilized liposomes and usually found water residues in a range of 7 to 8 % of their products. Therefore, secondary drying phase is necessary process to obtain complete dried lyophilized liposomes.

2.5.3.3 Secondary Drying Phase (Isothermal desorption)

Secondary drying phase will be operated after primary drying phase to eliminate water residues from matrix in dried lyophilized liposomes. In secondary drying phase, operation temperature (shelf temperature) should be higher than T_g', non-degradatio, and minimal value of pressure condition. The optimized secondary drying phase condition of lyophilization can be removed the water residues in dried lyophilized liposomes to lower than one percent. Therefore, secondary drying phase is an important factor of lyophilization leading to reduction of physicochemical instability of lyophilized liposomes.

2.5.4 Application of Liposomes

Figure 2.15 presented the encapsulation of various therapeutic agents of liposomes including hydrophilic drugs, hydrophobic drugs, polymeric system, DNA, RNA, siRNA, surface-conjugated drug, protein, and targeting ligand.

Nowadays, many studies revealed that liposomes can be utilized as a drug delivery system for treatment in several diseases such as cancer (Seetharamu et al., 2010), leishmaniasis (Shyam et al., 2010), fungal infection (Moen et al., 2009), wound recovery, (Fei et al., 2014), gene-associated disorder, and vaccine therapy (Schwendener RA., 2014). Table 2.4 also showed the liposomal products currently available in drug markets i.e Doxil® (anticancer drug), Myocet® (anticancer drug), and AmBisome® (antifungal drug).
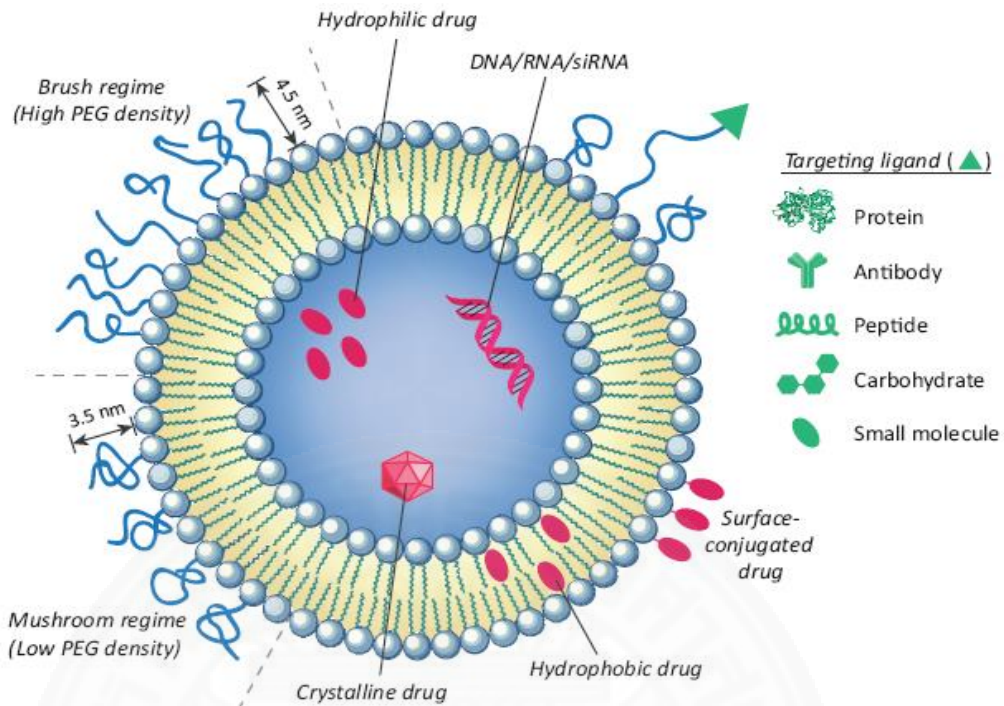
Figure 2.15 Encapsulation of therapeutic agents of liposomes.

Table 2.4 Advantages and liposomal formulations in available drug markets.

Advantage	Liposomal formulations
- Improvement of physicochemical properties	- Minoxidil, anthracyclines, peptides antibiotics, chelators, genes
- Increment of bioavailability	- Cortisones, doxorubicin, vasopressin
- Targeting drug delivery system	- Amphotericin B, vaccines, porphyrins
- Improvement of drug permeation	- Anesthetics, insulin, corticosteroids

2.5.5 Transportation of Liposomal Drug Delivery System

Figure 2.16 demonstrated the proposed transportation mechanism of liposomal drug delivery system which classified into four major mechanisms are (1) Adsorption: this mechanism is an essential pathway to transport the delivered drugs into intracellular membrane (passive diffusion drug uptake).

Generally, liposomes will be adsorbed onto cell surface by interact proteins of their structure leading to drug leakage of liposomes. After that, the delivered drugs will be surrounded on cell surface and then uptake into cytoplasm. (2) Endocytosis: liposomes will be interacted with partial compounds of cell surface. After that, liposomes will be transported into intracellular membrane by endosomes of cell membrane. Lysosomal enzymes in intracellular membrane will be interacted endosomes-liposomes complexes leading to drug leakage of liposomes into cytoplasm. (3) Fusion: lipid bilayer of liposomes will be interacted and fused with structure of cell membrane and then drug contents will be leaked into intracellular membrane. (4) Lipid exchange: phospholipid molecules between of liposomes and cell membrane will be exchanged their molecules leading to leakage of the delivered drugs into intracellular membrane.
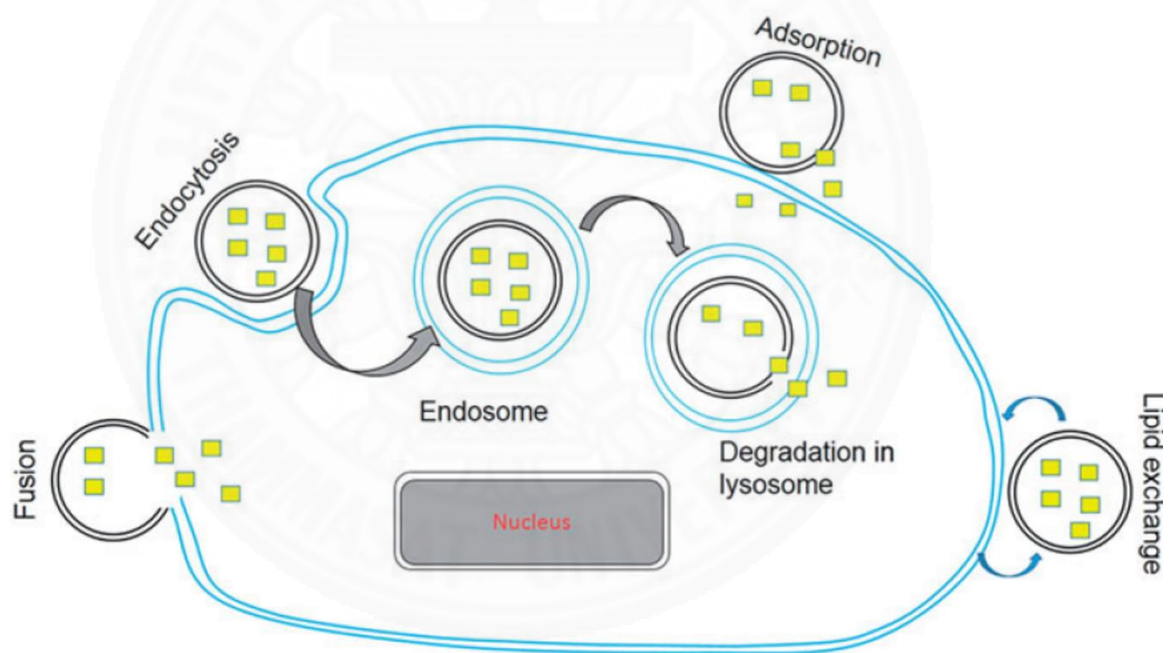
Figure 2.16 Transportation mechanism of liposomal drug delivery system.

CHAPTER 3
RESEARCH METHODOLOGY

3.1 Materials

3.1.1 Cholesterol (Lot No. K25236272849, Merck, Germany)

3.1.2 Dichloromethane (Lot No. 1L463001N, Carlo Erba Reagenti, Italy)

3.1.3 Di-sodium hydrogen orthophosphate anhydrous (Lot No. 0A708110E, Carlo Erba Reagenti, Italy)

3.1.4 Phosphatidylcholine (Lot No. 30510, Rhone-Poulenc Rorer, Germany)

3.1.5 Single chain polypeptide (Lot No. 20101004, Siam Bioscience, Thailand)

3.1.6 Sodium dihydrogen phosphate (Lot No. 0F047080I, Carlo Erba Reagenti, Italy)

3.1.7 Sodium hydroxide (Lot No. 1L216191N, Carlo Erba Reagenti, Italy)

3.1.8 Sucrose (Lot No. 0586978, ThermoFisher, UK)

3.2 Equipment

3.2.1 Centrifugation machine (Model 5403, Eppendorf, Germany)

3.2.2 Differential scanning calorimeter (Model DSC-800, Perkin Elmer, USA)

3.2.3 Freeze-dryer (Model FTS Systems, LyoStar^{TM}, USA)

3.2.4 Fourier transform infrared spectrometer (Model Nicolet iS50, Thermo-Fisher Scientific, USA)

3.2.5 High-speed centrifugation machine (Model RC6+, Sorvall®, USA)

3.2.6 Microscope (Model BH-2, Olympus, Japan)

3.2.7 pH-meter (Model S230, Mettler Toledo®, USA)

3.2.8 Precision electronic balance (Model AA-200DC, Denver Instrument, USA)

3.2.9 Reverse-phase high performance liquid chromatography (Model U3000, Dionex®, USA)

3.2.10 Rotary Evaporator (Model A-3S, Eyela®, Tokyo Rikakikai, Japan)

3.2.11 Scanning electron microscope (Model JSM-5410LV, Jeol, Japan)

3.2.12 Thermostatic cabinet (Model ST1+, Aquaterra®, Germany)

3.2.13 Transmission electron microscope (Model H-7000, Hitachi, Japan)

3.2.14 Ultra-low temperature freezers (Model S8600, Forma®, ThermoFisher Scientific, USA)

3.2.15 Ultrasonic bath (Model P410, Powersonic®, Hwashin Technology, Korea)

3.2.16 UV-spcetrophotometer (Model S18520-26, Secomam®, Thermolyne, USA)

3.2.17 X-ray diffractometer (Model D8 Advance, Bruker, Germany)

3.2.18 Zeta sizer (Model Nano-ZS, Malvern®, UK)

3.3 Methods

3.3.1 Preparation of SCP-LPs

SCP-LPs were prepared by reverse-phase evaporation technique (REV) at a molar ratio of phosphatidylcholine to cholesterol of 7:3. The phosphatidylcholine and cholesterol were dissolved in 60 mL of dichloromethane. Then, phosphate buffer saline solution (PBS) at pH 7.4 would introduce into lipid mixture solution with rapidly injection through a syringe needle. This mixture was immediately sonicated in the ultrasonic bath at 45 kHz, 25°C, and 15 minutes to obtain the water-in-oil emulsions (inverted micelles). The inverted micelles were evaporated by rotary evaporator for elimination of dichlorome-thane. This process was conducted under reduced pressure at 0.08 mPa with 35°C until the viscous gels were formed. The evaporation process would further continue for at least 30 minutes at 35°C to obtain liposomal dispersion. After that, liposomes were immediately sonicated at 45 kHz, 25°C, and 40 minutes to obtain uniform of liposome particles.

Then, SCP were loaded into liposomal dispersion and immediately sonic-ated at 45 kHz and 25°C with various sonication time intervals (0, 1, 3, and 5 minute(s) respectively) to obtain SCP-LPs. Finally, SCP-LPs were adjusted final volume by PBS.

3.3.2 Lyophilization of LSCP-LPs

The lyophilization of LSCP-LPs was performed at various freezing tempe-ratures i.e. -20°C, -40°C, and -80°C. Then, the optimized temperature was used for lyophi lization with variation of sucrose concentrations (sucrose as a cryoprotectant). They were investigated at molar ratio of SCP-LPs to sucrose of 1:0, 1:1, 1:3, and 1:5.

3.3.3 Characterization of SCP-LPs and LSCP-LPs

3.3.3.1 Evaluation of Physicochemical Properties of SCP-LPs and LSCP-LPs

(1) Measurement of Particle Size and PDI of SCP-LPs and LSCP-LPs

The photon correlation spectroscopy technique (PCS) was used to determine particle diameter and polydispersity index (PDI) of SCP-LPs and LSCP-LPs. Briefly, 1 mL of sample was transfer into cuvette and conducted under fluctuation rate in laser light scattered of 90° and 25°C. All samples were measured in 3 replicates and reported in a form of mean±standard deviation (SD).

(2) Measurement of Zeta Potential of SCP-LPs and LSCP-LPs

The laser doppler micro-electrophoresis technique was used for eva-luation of zeta potential of SCP-LPs and LSCP-LPs by using Zeta sizer. Briefly, 1 mL of sample was injected into folded capillary cell. After that, electrical energy was applied into their sample and then calculated their particle velocity for conversion of zeta potential of sample. All samples were measured in triplicates and reported in a form of mean±SD.

(3) Determination of Drug Entrapment Efficiency of SCP-LPs and LSCP-LPs

Unbound SCP of SCP-LPs and LSCP-LPs were separated by high-speed centrifugation machine at 47,000×g, 4°C, for 60 minutes.

After that, the amount of unbound SCP was determined by reverse phase-high performance liquid chromatography technique (RP-HPLC) with gradient program using zorbax eclipse columns (C18, 80 Å, LC column 250x4.6 mm). The mobile phases consisted of 70% to 30 % of 0.1% trifluoroacetic acid in water and 0.1% trifluoroacetic acid in acetonitrile at flow rate of 1.0 mL/min. SCP was detected by ultraviolet detector at a wavelength of 280 nm. All samples were analyzed in 3 replicates and reported in a form of mean±SD.

The amount of SCP of sample was calculated from different values of an amount of SCP added into liposomes (A) and the amount of unbound SCP in the supernatant after centrifugation (B).

SCP entrapment efficiency was calculated by using equation (1).

$$\text{Percent of drug entrapment efficiency} = \frac{(A\text{-}B)\times100}{A} \qquad (1)$$

3.3.4 Morphological Observation of LSCP-LPs

3.3.4.1 Scanning Electron Microscopy (SEM)

The morphology of LSCP-LPs at various molar ratios of SCP-LPs to sucrose of 1:0, 1:1, 1:3, and 1:5 were investigated by SEM. Briefly, sample was dropped on a cover slip and dehydrated with desiccator at ambient temperature to obtain dried sample. After that, sample was applied on osmium oxide vapor. Finally, sample was coated with thin layer of gold.

3.3.4.2 Transmission Electron Microscopy (TEM)

TEM was used to investigate morphology of LSCP-LPs at varied molar ratios of SCP-LPs to sucrose of 1:0, 1:1, 1:3, and 1:5. Briefly, sample was diluted with sterile water and then dropped on copper grid with carbon film. After that, sample was stained with 0.5% uranyl acetate to generate negatively charge of sample. Finally, sample was dehydrated with desiccator at ambient temperature.

3.3.5 X-Ray Powder Diffraction Analysis (XRD) of LSCP-LPs

XRD was employed to determine chemical interaction of composition molecules in LSCP-LPs. This analysis was performed under radiation sources of CuK_{α}, 2-Theta scanning range at 5 to 50°, and scanning rate of 1°/min.

3.3.6 Thermal Analysis of LSCP-LPs

The chemical interaction of ingredient molecules of LSCP-LPs was used thermal analysis. This analysis was determined by differential scanning calorimetry technique (DSC). Briefly, sample was weighed in a range of 5 to 10 mg in aluminum pan and conducted under temperature range of -100 to 300°C, flow rate of nitrogen gas of 25 mL/min, and heating rate of 5°C/min.

3.3.7 Fourier Transform-Infrared Spectroscopy Analysis (FT-IR) of LSCP-LPs

FT-IR was applied to evaluate chemical interaction and functional group of composition molecules of LSCP-LPs. This technique was performed under attenuated total reflection mode (ATR), wavelength range of 500 to 4000 nm, and signal average of 30 scans.

3.3.8 Stability Evaluation of SCP-LPs, LSCP-LPs, and RSCP-LPs

Stability evaluation of SCP-LPs, LSCP-LPs, and reconstituted SCP-loaded liposomes (RSCP-LPs) were conducted. The test products were kept in either refrigerator (2 to 8°C) and ambient (25±1°C) temperature conditions with light protection for a month. All sample was evaluated their physicochemical properties such as particle size, PDI, zeta potential, and drug entrapment efficiency at day 0, 7, 14, 21, and 30.

3.3.9 *In Vitro* Drug Release Study of LSCP-LPs

The *in vitro* drug release study of LSCP-LPs was investigated by using modified Franz diffusion cells. The receptor compartment containing PBS as receiving media was separated from donor compartment by cellulose acetate membrane. It was maintained at the temperature of 37±1°C and continuously stirred at 50 RPM throughout the study. The 3 mL of receiving media was taken for chemical analysis of SCP by using RP-HPLC at 0.00, 0.08, 0.25, 0.5, 1, 2, 3, 4, 5, 6, 7, and 8 hour(s).

3.3.10 *In Vitro* Eye Irritation Test of LSCP-LPs

The *in vitro* eye irritation test of LSCP-LPs was evaluated by MTT (3-(4,5-dimethylthiazol-2-yl)-2,5-diphenylte-trazolium bromide) assay. Briefly, SIRC cells were inoculated into Eagle's minimum essential medium (EMEM) and seeding in 24-well plates. After that, SIRC cells were incubated with reconstituted LSCP-LPs at concentration of either 0.05% and 5% for 5 mins according to short time exposure test (STE) and then washed with PBS (pH 7.4). MTT reagent was added to media of sample and incubated for 2 hrs. After that, MTT formazan was extracted and analyzed by microplate reader at a wave length of 570 nm. Finally, their optical density value was calculated a percentage of cell viability (%CV) and then scored eye irritation potential for LSCP-LPs.

3.3.11 *In Vitro* Cell Proliferation-Promoting Activity Test of LSCP-LPs

MTT assay was used to determine *in vitro* cell proliferation promoting activity test of LSCP-LPs. SIRC cells were incubated with 5% reconstituted LSCP-LPs and 5% empty liposomes in media for 24 hours and washed with PBS at pH 7.4. Then, MTT reagent was loaded into media of sample and incubated for 2 hrs. After that, MTT formazan was extracted and analyzed by microplate reader at a wavelength of 570 nm.

3.3.12 Statistical Analysis

The obtained data were statistically analyzed (ANOVA and paired t-test) by using SPSS program at a significant level of 0.05.

CHAPTER 4
RESULTS AND DISCUSSION

4.1 Characterization and Evaluation of Physicochemical Properties of SCP-LPs

4.1.1 The Effect of Sonication Time of SCP-LPs
4.1.1.1 Measurement of Particle Size and PDI of SCP-LPs

The particle size of SCP-LPs was in a range of nanometer (around 81 to 88 nm) with narrow particle size distribution. Their PDI values were 0.22-0.23. Table 4.1 revealed that the particle size of SCP-LPs was affected by sonication time. The sonication time of 5 minutes were selected. Because this sonication time could reduce particle size of SCP-LPs to smallest diameter. In addition, their particle size was significantly decreased with increase of sonication time (p-value <0.05). Therefore, this sonication time was selected for further study. This is due to the fact that energy supplied by ultrasonic waves (mechanic forces) could stimulate phospholipid molecules in the lipid bilayer of SCP-LPs leading to disordered lipid bilayer conformation and then smaller particle size of SCP-LPs were obtained (Akbarzadeh et al., 2013). In addition, ultrasonic waves could interact microbubbles of air in aqueous phase leading to oscillation of microbubbles called cavitation. Moreover, ultrasonic waves induced implosion of microbubbles by stimulating expansion and contraction of their structure. This phenomenon could induce large particles of SCP-LPs to smaller SCP-LPs. Generally, small liposomes could exhibit highly potential for increment of bioavailability profile of the delivered drug. A similar finding, previous research of Li et al. (2009) revealed that the appropriate particle diameter of chitosan-coated with diclofenac-loaded liposomes could increase corneal permeation, precorneal retention time, reduction of cytotoxicity, and resulting in higher ophthalmic bioavailability. In addition, Wang et al. (2010) reported that the nanoparticles of folate-PEG coated polymeric liposomes also showed higher efficiency for cellular uptake of folate into cancer cells when comparing with multilamellar liposomes.

Moreover, Immordino et al. (2006) demonstrated that the small unilamellar liposomes had stealth property. Their property could avoid opsonization from white blood cells (macrophage) leading to increment of half-life of their particles in blood circulation system.

4.1.1.2 Measurement of Zeta Potential of SCP-LPs

Zeta potential values of SCP-LPs were in a range of -1 to -3 mV. Table 4.1 reported that zeta potential of SCP-LPs was affected by sonication time. The sonication time of 5 minutes were selected. Because this sonication time exhibited that in the highest negative charge value. Moreover, their zeta potential of SCP-LPs was significantly decreased with increase of sonication time (p-value <0.05). Therefore, this sonication time was selected for further study. This is due to the fact that the ultrasonic energy could accelerate SCP for embedment of SCP in lipid bilayer of SCP-LPs leading to increment of their zeta potential. In addition, ultrasonic waves could reduce rigidity of lipid bilayer of SCP-LPs leading to increase of SCP entrapment efficiency of SCP-LPs (Yin et al., 2014). Moreover, the increment of zeta potential of liposomes could induce high bioavailability profile of the delivered drug and increase their physical stability. Vural et al. (2011) demonstrated that the nano-complexes of furosemide-loaded liposomes with higher surface charge could eight-fold increase furosemide permeability into cells when comparing with their particles with lower surface charge. In addition, high surface charge of nanocomplex of furosemide-loaded liposomes demonstrated that in low cytoto-xicity. A similar finding, Han et al. (2012) reported that alendronate-loaded liposomes with high zeta potential exhibited that their particle had strong muco-adhesive properties in bio-logical cells with 2.6-fold enhancement for cellular uptake of alendronate. Moreover, increment of zeta potential of liposomes could improve physical instability by using electrostatic interaction in their surface structure. A similar finding, previous reported of Hanaor et al. (2012) demonstrated that higher zeta potential of liposomal products could increase physical stability in the colloidal system when comparing with their particles with lower zeta potential.

4.1.1.3 Determination of Drug Entrapment Efficiency of SCP-LPs

The drug entrapment efficiency of SCP-LPs prepared in this study were in a range of 23 to 97%. Table 4.1 revealed that the drug entrapment efficiency of SCP-LPs was affected by sonication time. The more sonication time and drug entrapment efficiency, because of sonication time of 5 minutes provided highest drug entrapment efficiency of liposomes, it was selected for further study. In addition, their drug entrapment efficiency was significantly increased with increase of sonication time compared to non-sonicated SCP-LPs (p-value <0.05). Therefore, this sonication time was selected for further study. As described in Topic 4.1.1.2, ultrasonic waves could rearrange orientation in lipid bilayer of liposomes structure and increase embedment of SCP in their lipid bilayer of SCP-LPs. Moreover, ultrasonic waves could reduce rigidity of lipid bilayer of SCP-LPs leading to increase of SCP entrapment efficiency of SCP-LPs. A similar finding, Yin et al. (2014) reported that the SCP entrapment efficiency of SCP-LPs with sonication technique could induce highly SCP entrapment efficiency more than 90%. Moreover, Alipour et al. (2008) revealed that Polymyxin B-loaded liposomes with sonication technique demonstrated that their particles had higher Polymyxin B entrapment efficiency when comparing with Polymyxin B-loaded liposomes from filter extrusion technique.

Table 4.1 Physicochemical properties of SCP-LPs with various sonication time intervals (n= 3; Mean±SD).

Sonication time (minute(s))	Particle size (nm)	PDI	Zeta potential (mV)	Drug entrapment efficiency (%)
0	88.59±0.12	0.23±0.00	-1.13±0.14	23.54±0.93
1	87.87±0.03	0.23±0.00	-2.27±0.07	35.45±1.12
3	84.84±0.07	0.23±0.00	-2.46±0.02	93.69±1.04
5	81.12±0.09	0.22±0.00	-2.95±0.04	97.56±0.85

4.2 Characterization and Evaluation of Physicochemical Properties of LSCP-LPs

4.2.1 The Effect of Solidification (Freezing phase) of LSCP-LPs
4.2.1.1 Measurement of Particle Size and PDI of LSCP-LPs

The particle size of LSCP-LPs was in a range of nanometer (approximately 82 to 109 nm) with acceptance particle size distribution. Their PDI values were 0.3 to 0.4. Table 4.2 reported that the particle size of LSCP-LPs was affected by freezing temperature. The freezing temperature at -40°C was considered as an optimum freezing temperature, because the obtained liposomes had the smallest particle size. In addition, this freezing temperature did not show statistical significance (p-value <0.05) of particle size and PDI of LSCP-LPs when comparing with SCP-LPs. Therefore, this freezing temperature was selected for further study. As described in Topic 2.6.1, unsuitable freezing temperature for solidification of liposomal products caused the unsuitable freezing rate and then induced physical instability of lyophilized liposomal products. This is due to the fact that unsuitable freezing rate could increase the formation of dendritic ice crystal. They could penetrate and attack liposomal structure leading to drug leakage from liposomes and liposomal vesicle aggregation. In addition, Kasper et al. (2011) reported that the appropriate freezing rate was preferred for lyophilization in liposomal products more than too slow and too rapid freezing rate. Because appropriate freezing rate would generate few amount of dendritic ice crystals leading to reduction of degradation of lyophilized liposomal products. A similar finding, Aso et al. (2005) revealed that unsuitable freezing temperature of solidification of liposomal products could increase their particle diameter and could induce physical instability in their long-term storage condition.

4.2.1.2 Measurement of Zeta Potential of LSCP-LPs

Zeta potential values of LSCP-LPs were in a range of -2 to -3 mV. Table 4.2 revealed that zeta potential of LSCP-LPs was affected by freezing temperature. However, the freezing temperature of -40°C was selected become for further study, because this freezing temperature provided the highest zeta potential value of LSCP-LPs.

In addition, the zeta potential of LSCP-LPs prepared at this freezing temperature was not significant difference (*p*-value <0.05) from that of SCP-LPs. As described in Topic 4.2.1.1, unsuitable freezing temperature of solidification would generate unsuitable freezing rate leading to leakage of SCP from LSCP-LPs. This phenomenon would reduce zeta potential of LSCP-LPs. Moreover, the unsuitable freezing rate would generate many stress conditions of solidification from high matrix mobility and dendritic ice crystal formation leading to physical instability of LSCP-LPs (Kasper et al., 2011).

4.2.1.3 Determination of Drug Entrapment Efficiency of LSCP-LPs

The drug entrapment efficiency of LSCP-LPs prepared in this study were found in a range of 46 to 73%. Table 4.2 reported that the drug entrapment efficiency of LSCP-LPs frozen at a temperature of -20°C and -80°C had lower drug entrapment efficiency when comparing with LSCP-LPs frozen at -40°C. Therefore, this freezing temperature was selected for further study. As described in Topic 4.2.1.1, unsuitable freezing rate could increase dendritic ice crystal formation. Then, dendritic ice crystals would penetrate and destroy liposomal structure leading to reduction of SCP entrapment efficiency in LSCP-LPs.

Table 4.2 Physicochemical properties of LSCP-LPs with various freezing temperatures (*n*=3; Mean±SD).

Freezing temperature (°C)	Particle size (nm)	PDI	Zeta potential (mV)	Drug entrapment efficiency (%)
SCP-LPs	81.12±0.09	0.22±0.00	-2.95±0.04	97.56±0.85
-20	89.54±0.21	0.28±0.00	-2.03±0.02	45.54±0.38
-40	81.56±0.13	0.23±0.00	-2.90±0.03	73.28±0.93
-80	108.93±0.15	0.43±0.00	-1.94±0.03	65.46±0.22

4.2.2 The Effect of Cryoprotectant Concentration of LSCP-LPs

4.2.2.1 Measurement of Particle Size and PDI of LSCP-LPs

The particle size of LSCP-LPs prepared in this study was in a range of nanometer around 81 to 1829 nm. Most of them had PDI values around 0.2 to 0.4 except for the formulation without cryoprotectant, the obtained liposomes had PDI value more than 1.0. Table 4.3 revealed that the particle size and PDI of LSCP-LPs were affected by sucrose concentration. The LSCP-LPs (1:5) were selected, because this molar ratio provided the smallest particle diameter with the narrowest size distribution. These values were not statistically different from SCP-LPs (p-value <0.05).

This finding could be explained that sucrose molecule interacts with hydrophilic head of phospholipid molecule of SCP-LPs via hydrogen bonding and then replace water molecules in lipid bilayer of SCP-LPs. The unsubstituted sucrose could generate glassy matrix (amorphous organization of sucrose) surround the liposomes. These phenomena could prevent particles aggregation during solidification process leading to insignificantly change in their physicochemical properties. A similar finding, Ohshima et al. (2009) revealed that cryoprotective agents could protect liposomal structure of lyophilized nifedipine loaded-liposomes from vesicle aggregation. Moreover, their reconstituted products could be redispersed more easily than that of the formulation without addition of cryoprotectants. Wang et al. (2009) also reported that the appropriate cryoprotectant concentration could maintain particle size and drug entrapment efficiency of reconstituted polymyxin E sulfate-loaded liposomes.

4.2.2.2 Measurement of Zeta Potential of LSCP-LPs

Zeta potential values of LSCP-LPs were in a range of -2 to -3 mV. Table 4.3 reported that zeta potential of LSCP-LPs was affected by sucrose concentration. The LSCP-LPs (1:5) were selected, because this molar ratio provided the highest zeta potential value of LSCP-LPs. However, LSCP-LPs (1:5) did not cause significant difference (p-value <0.05) in their zeta potential compared with SCP-LPs. Therefore, this molar ratio was selected for further study.

As described in Topic 4.2.2.1, unsuitable sucrose concentration did not generated sufficient amorphous matrix to covered and protected their particles from stress during solidification process. This phenomenon could induce reduction of zeta potential of LSCP-LPs. A similar finding, previous research of El-Nesr et al. (2010) reported that lyophilized fluconazole-loaded liposomes without addition of cryoprotective agents could influence low zeta potential leading to physical instability. Moreover, their liposomal product without addition of cryoprotective agent could not be redispersed homogeneously after reconstitution when comparing with the formulation containing cryo-protectant.

4.2.2.3 Determination of Drug Entrapment Efficiency of LSCP-LPs

The drug entrapment efficiency of LSCP-LPs prepared in this study were in a range of 32 to 73%. Table 4.3 revealed that the drug entrapment efficiency of LSCP-LPs was affected by sucrose concentration. The LSCP-LPs (1:5) were selected, because this molar ratio provided the highest drug entrapment efficiency of LSCP-LPs. Therefore, this molar ratio was selected for further study. This is due to the fact that unsui-table sucrose concentration could not be protected liposomal structure from dendritic ice crystal formation which described in Topic 4.2.2.2. This phenomenon could induce SCP leakage from LSCP-LPs during solidification (Gregoriadis, 2016).

Table 4.3 Physicochemical properties of LSCP-LPs with various cryoprotectant concen-trations (n=3; Mean±SD).

Cryoprotectant concentration (Molar ratio)*	Particle size (nm)	PDI	Zeta potential (mV)	Drug entrapment efficiency (%)
SCP-LPs	81.12±0.09	0.22±0.00	-2.95±0.04	97.56±0.85
LSCP-LPs (1:0)	1829.00±2.00	Not detected	-1.95±0.03	31.63±0.47
LSCP-LPs (1:1)	92.91±0.06	0.39±0.00	-2.26±0.04	32.67±0.42
LSCP-LPs (1:3)	85.50±0.29	0.27±0.00	-2.38±0.03	56.22±0.36
LSCP-LPs (1:5)	81.56±0.13	0.23±0.00	-2.90±0.03	73.28±0.93

*Molar ratio of SCP-LPs to sucrose

4.3 Morphological Observation of LSCP-LPs

4.3.1 Scanning Electron Microscopy (SEM)

SEM technique was the necessary technique for investigation of morphology and surface topography of nanomaterials. Figure 4.1 in **(a)**, **(b)**, and **(c)** present the morphology of LSCP-LPs (1:0), LSCP-LPs (1:1), and LSCP-LPs (1:3) respectively. They revealed that these liposomes had heterogenous particle size with irregular morphology. In addition, aggregation of liposome vesicles was found as well. This finding was consistent with the results of particle size and PDI determination of LSCP-LPs in Table 4.3. However, Figure 4.1 in **(d)** present morphology of LSCP-LPs (1:5) revealed that the SEM photomicrograph of LSCP-LPs had spherical shape with particle size in nanometer range consistent with the results of particle size and PDI determination of LSCP-LPs in Table 4.3. Therefore, SEM photomicrographs of LSCP-LPs could confirm that appropriate sucrose concentration could stabilize liposomal structure during lyophilization. As described in Topic 4.2.2.1, suitable sucrose concentration could protect structure of liposomes from stress during lyophilization. A similar finding, Chaudhury et al. (2012) reported that the SEM photomicrographs of cholesterol-free PEGylated liposomes with optimized cryoprotectant concentration had spherical shape and acceptable particle size. In addition, Jangle et al. (2013) revealed that the suitable sucrose concentration in curcumin-loaded liposomes had appropriate particle diameter and showed spherical shape.
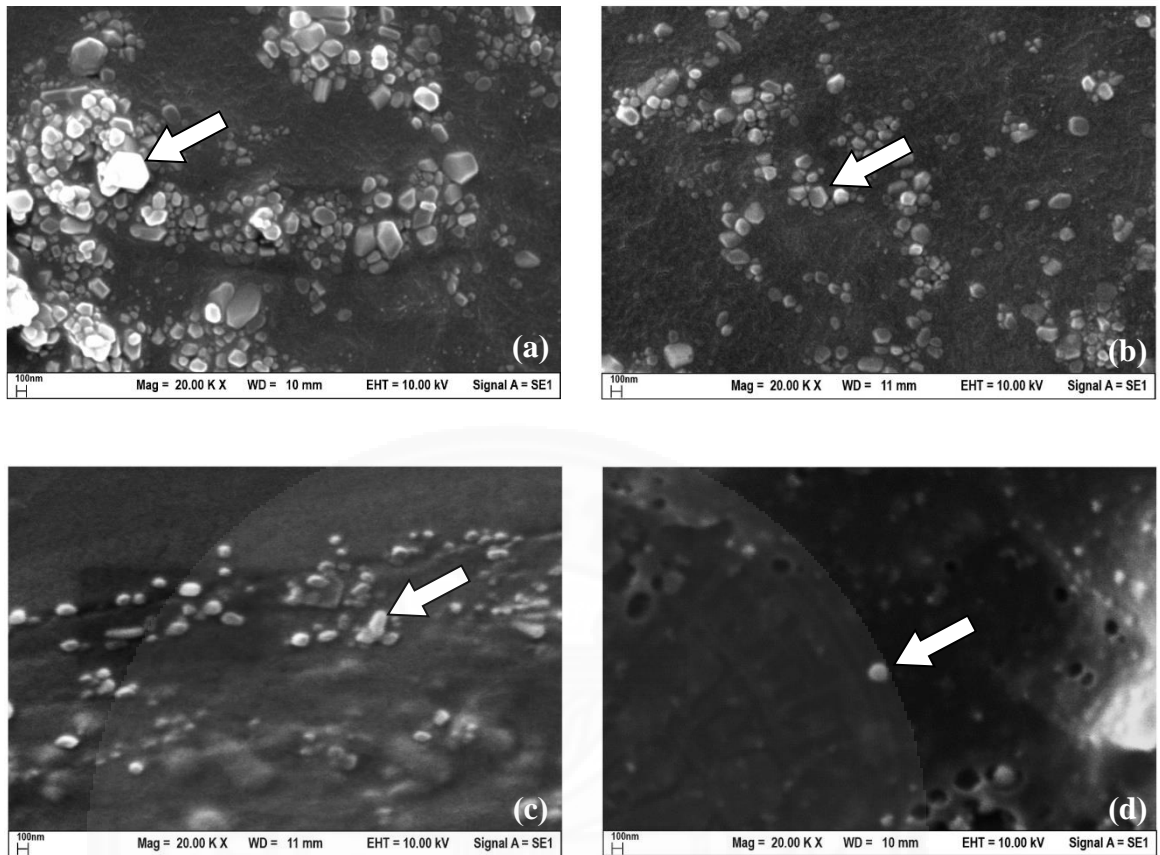
Figure 4.1 SEM photomicrographs of LSCP-LPs **(a)** LSCP-LPs (1:0), **(b)** LSCP-LPs (1:1), **(c)** LSCP-LPs (1:3), and **(d)** LSCP-LPs (1:5) respectively.

4.3.2 Transmission Electron Microscopy (TEM)

TEM is one of essential techniques to investigate morphology and classify liposome vesicles of LSCP-LPs. Figure 4.2 in (a), (b), and (c) present the morphology LSCP-LPs $(1:0)$, LSCP-LPs $(1:1)$, and LSCP-LPs $(1:3)$ respectively. They revealed that the liposomes with unsuitable sucrose concentrations would be surrounded with large lipid vesicle with various particle size, and aggregated vesicles. In addition, this finding was consistent with the results of particle size and PDI determination of LSCP-LPs in Table 4.3. However, Figure 4.2 in (d) present morphology of LSCP-LPs $(1:5)$ represented that they had appropriate of particle diameter with spherical shape

Thus, all TEM photomicrographs of LSCP-LPs insisted that appropriate sucrose concentration could prevent liposomal structure of LSCP-LPs during lyophilization. This phenomenon was described in Topic 4.2.2.1.
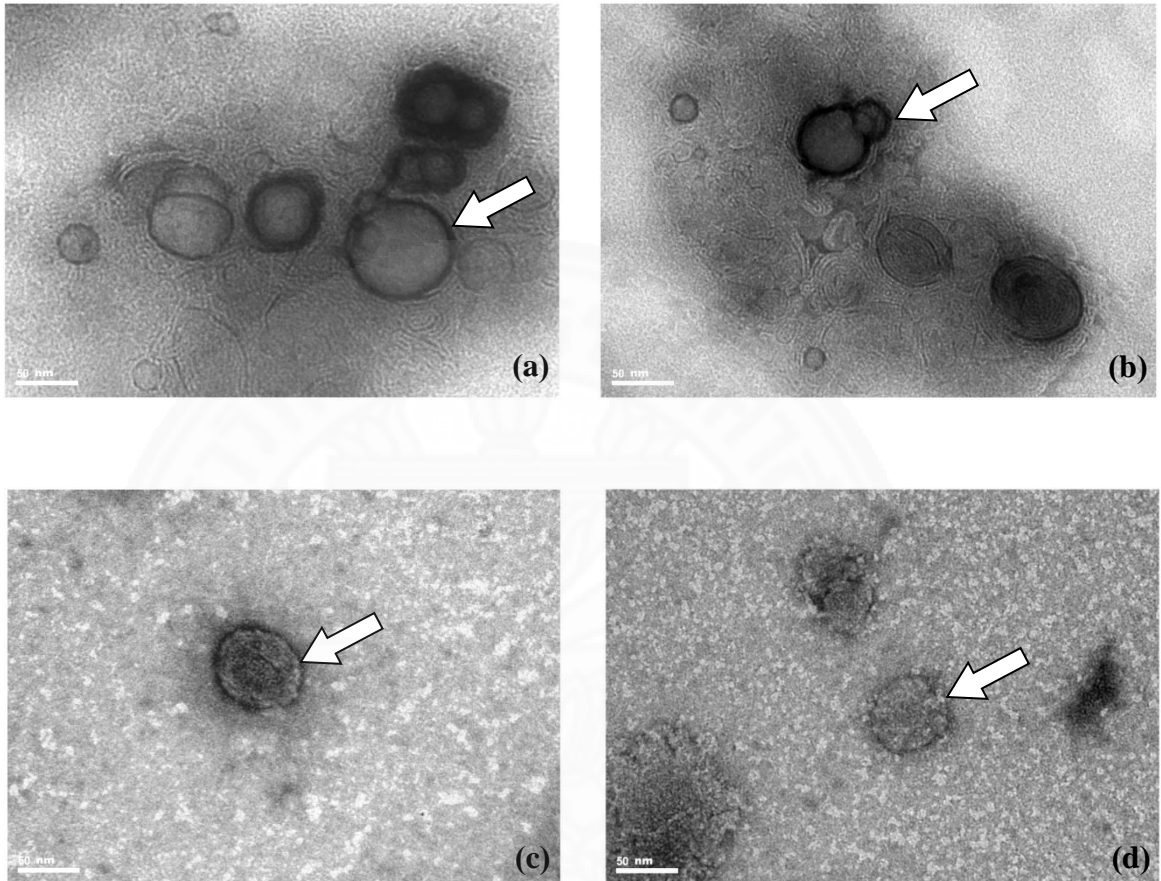
Figure 4.2 TEM photomicrographs of LSCP-LPs **(a)** LSCP-LPs (1:0), **(b)** LSCP-LPs (1:1), **(c)** LSCP-LPs (1:3), and **(d)** LSCP-LPs (1:5) respectively.

4.4 X-Ray Powder Diffraction Analysis (XRD) of LSCP-LPs

XRD analysis is commonly used to investigate chemical interactions of compositions containing in liposomal formulations.
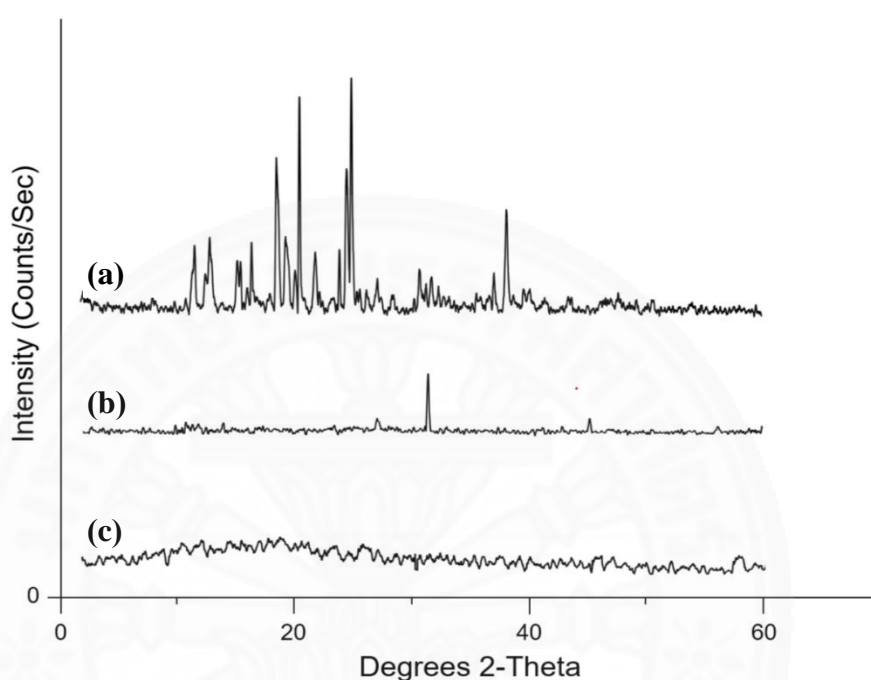
Figure 4.3 Diffractograms: **(a)** physical mixture, **(b)** SCP, and **(c)** LSCP-LPs respectively.

Figure 4.3 in **(a)**, **(b)**, and **(c)** showed diffractograms of physical mixture of phosphatidylcholine, cholesterol, SCP, and sucrose), SCP, and LSCP-LPs respectively. They revealed that most of the compositions in the physical mixture were in crystalline form while the compositions in the liposomes were in the amorphous form. This might be due to the chemical interaction between compositions of LSCP-LPs leading to new specific ordered organization. This phenomenon suggested that some of SCP dispersed in the liposomal structure of LSCP-LPs. A similar finding in previous research reported by Cabral et al. (2004) revealed that diffractogram of lyophilized allergenic protein-loaded liposomes had the broad of peak (halo pattern) when comparing with diffractograms of the pure compounds.

In addition, the broad of the peak of lyophilized allergenic protein-loaded liposomes indicated that their compositions were arranged and converted into new chemical interactions with amorphous characteristic. Moreover, Liu et al. (2012) reported that the diffractogram of polycaprolactone-loaded liposomes would be broader peak when comparing to diffractogram of polycaprolactone bulk drug. These results indicated that polycaprolactone would less ordered of crystallinity leading to amorphous organization because of dispersion of polycaprolactone in structure liposomes.

4.5 Thermal Analysis of LSCP-LPs

This study was performed to determine chemical interactions between compositions in liposomal formulations and physicochemical property of LSCP-LPs. Figure 4.4 in **(a)**, **(b)**, and **(c)** presented the thermograms of physical mixture, SCP, and LSCP-LPs respectively. Figure 4.4 in **(c)** indicated that LSCP-LPs had lower melting temperature compared to with thermograms of physical mixture and SCP respectively (Figure 4.4 in **(a)** and **(b)**). Their precise values of melting temperature and melting enthalpy were shown in Table 4.4. It was found that the melting temperature and melting enthalpy of LSCP-LPs < SCP < the physical mixture. This could be explained the compositions of LSCP-LPs were rearranged into amorphous organization. This phenomenon was usually found in various nanocomplexes (Chime et al., 2013). A similar finding, Charnvanich et al. (2010) reported that thermogram of lysozyme-loaded liposomes had lower melting temperature and melting enthalpy compared to these of pure materials.

These findings suggested that there were interactions between the formulation composition. Yoshida et al. (2010) showed the thermogram of essential oil-loaded liposomes having lower melting temperature compared to pure compounds. Therefore, their melting process of essential oil-loaded liposomes implied that the essential oils could disperse in liposomal structure of their particles.
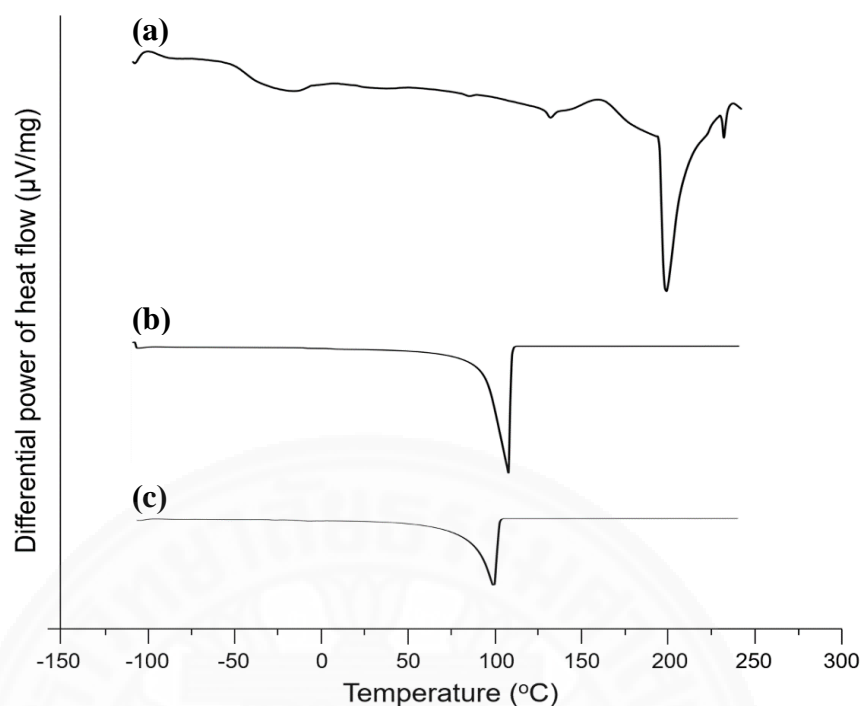
Figure 4.4 Thermograms: **(a)** physical mixture, **(b)** SCP, and **(c)** LSCP-LPs respectively.

Table 4.4 Thermal analysis of physical mixture, SCP, and LSCP-LPs (*n*=3; Mean±SD).

Materials/Formulation	Melting temperature (°C)	Melting enthalpy (J/g)
Physical mixture	205.79±0.12	145.62±0.04
SCP	115.55±0.09	109.85±0.13
LSCP-LPs	107.29±0.03	78.23±0.07

4.6 Fourier Transform-Infrared Spectroscopy Analysis (FT-IR) of LSCP-LPs

Although, XRD and thermal analysis were the essential techniques to investigate chemical interaction in compositions of LSCP-LPs but their techniques could not be identified and less information of functional group of chemical interactions between the compositions of LSCP-LPs. Figure 4.5 in **(a)**, **(b)**, and **(c)** presented the FT-IR spectra of SCP, LPs, and LSCP-LPs respectively. Figure 4.5 in **(c)** revealed that the FT-IR spectrum of LSCP-LPs were absence peaks in the wavenumbers of 2800 to 2900 cm^{-1} (assigned

to -CH stretching: hydrocarbon group) and 1720 to 1740 cm^{-1} (assigned to -C=O stretching: saturated aldehyde or carbonyl group) when comparing with FT-IR spectrum of empty liposomes (Figure 4.5 in **(b)**). This is due to the fact that the hydrocarbon and aldehyde groups in fatty acid chain of phosphatidylcholine of LSCP-LPs were embedded and interacted with partial structure of SCP. Moreover, the FT-IR spectrum of LSCP-LPs had the specific peak in the wavenumber of SCP at 1647 cm^{-1} which this wavenumber assigned to random coil structure type of secondary structure of SCP (Yang et al., 2004). However, FT-IR spectrum band of empty liposomes (Figure 4.5 in **(b)**) did not appeared this peak. In addition, Figure 4.5 in **(c)** revealed that the FT-IR spectrum of LSCP-LPs had higher broad of peak in the wavenumbers of 3200 to 3600 cm^{-1} (assigned to -OH bending: hydroxyl group) when comparing with FT-IR spectra of SCP and LPs (Figure 4.5 in **(a)** and **(b)**). Because SCP provided hydroxyl group of their structure to LSCP-LPs leading to increment of hydroxyl group of LSCP-LPs. Therefore, all phenomena implied that SCP could substitute their structure into lipid bilayer of LSCP-LPs. A similar finding, the results of diffractogram and thermogram of LSCP-LPs demonstrated that the SCP could be incorporated and dispersed in the liposomal structure of LSCP-LPs.
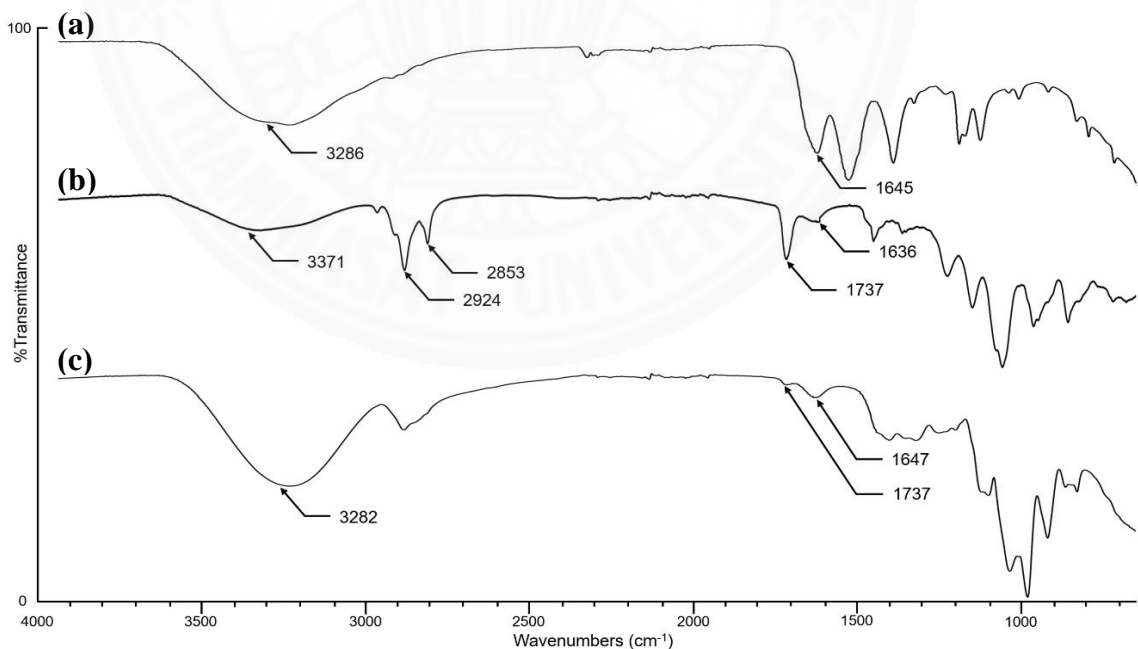
Figure 4.5 FT-IR spectra: **(a)** SCP, **(b)** empty liposomes, and **(c)** LSCP-LPs respectively.

4.7 Stability Evaluation of SCP-LPs, LSCP-LPs, and RSCP-LPs

Stability evaluation of SCP-LPs, LSCP-LPs, and RSCP-LPs could classify into two groups were 1) refrigerator temperature condition (0 to 4°C) and 2) ambient temperature condition (25±1 °C). During the study, they were protected from light for a month. All samples were evaluated for their particle size, PDI, zeta potential, and drug entrapment efficiency at day 0, day 7, day 14, day 21, and day 30.

Figure 4.6 to 4.9 presented the results of stability evaluation of SCP-LPs, LSCP-LPs, and RSCP-LPs. It was found that LSCP-LPs kept at at 4°C did not show significant difference (p-value <0.05) in their particle size, PDI, zeta potential, and drug entrapment efficiency from those of LSCP-LPs at the initial day. Therefore, thie condition could be accepted as the optimum storage condition for LSCP-LPs.

Moreover, LSCP-LPS at 4°C demonstrated that the lyophilized liposomal products had higher physical stability than that of SCP-LPs and RSCP-LPs at 4°C. This may be due to the fact that the aqueous part of liposomal products causing destabilization of their physicochemical properties by hydrolysis reaction was removed. Because water molecules in liposomal products interacted with phospholipid molecules in SCP-LPs and RSCP-LPs, it could induce liposomal degradation such as vesicle aggregation, lower zeta potential, and drug leakage. This finding was consistent with Ghanbarzadeh et al. (2013) demonstrated that lyophilized sirolimus-loaded liposomes had higher physicochemical properties (included particle size and drug leakage) when comparing to non-lyophilized liposomes for 6 months.

Although, lyophilized liposomal products had higher physical stability than liposomal products in dispersed aqueous vehicles. However, the essential factors for improvement of shelf-life of liposomal products was a storage temperature. It was found that SCP-LPs, LSCP-LPs, and RSCP-LPs kept at 25°C showed obvious physical instability. All formulations kept under storage temperature at 25°C had significant difference (p-value <0.05) in their physicochemical properties compared to those of them at the initial day.

This finding could be explained that high temperature disturbed the orientation of phosphatidylcholine in lipid bilayer leading to disordered conformation and then flexibility and permeability of liposomal bilayer were increased (Ming et al., 2013).

The previous study by Muppidi et al. (2012) revealed that bulk lyophilized vancomycin-loaded liposomes and non-lyophilized vancomycin-loaded liposomes were stable at 4°C for 3 months. Moreover, they did not show significant change in their physico-chemical properties i.e. particle diameter, particle size distribution, and drug entrapment efficiency, compared to those of formulations kept at 37°C.
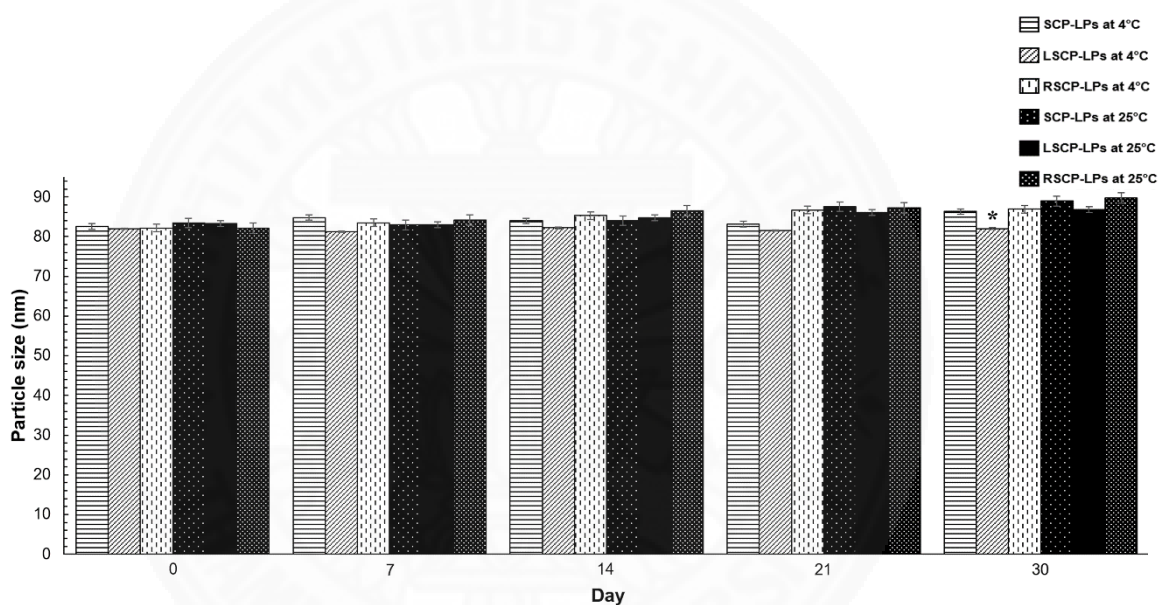
Figure 4.6 Particle size of SCP-LPs, LSCP-LPs, and RSCP-LPs at day 0, day 7, day 14, day 21, and day 30 respectively (*n*= 3; Mean±SD), *insignificantly different from day 0 (p-value <0.05).
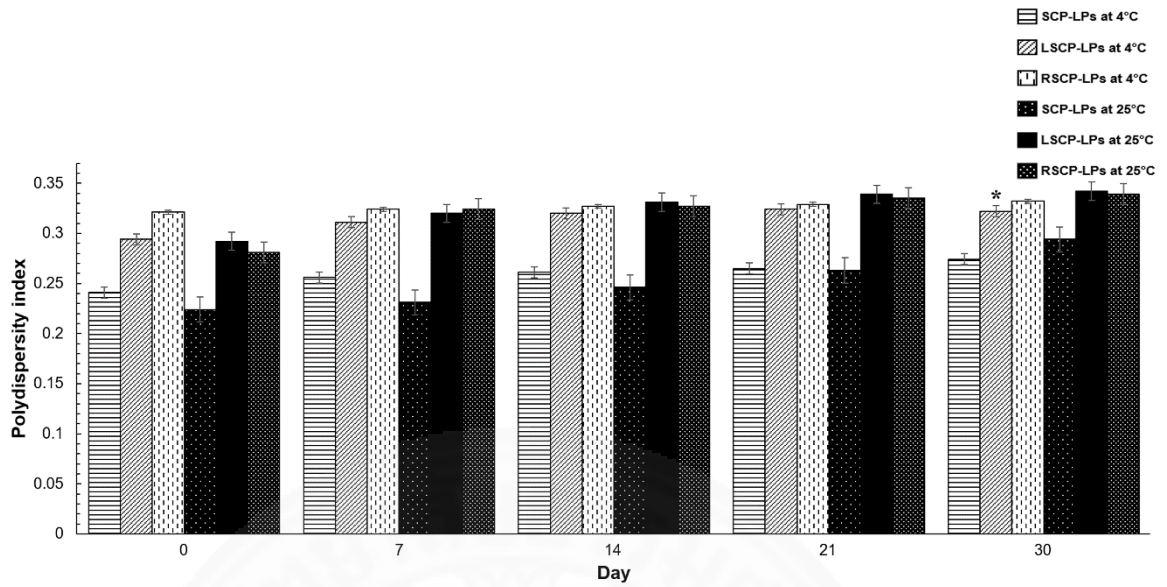
Figure 4.7 PDI of SCP-LPs, LSCP-LPs, and RSCP-LPs at day 0, day 7, day 14, day 21, and day 30 respectively (*n*= 3; Mean±SD) *insignificantly different from day 0 (p-value <0.05).
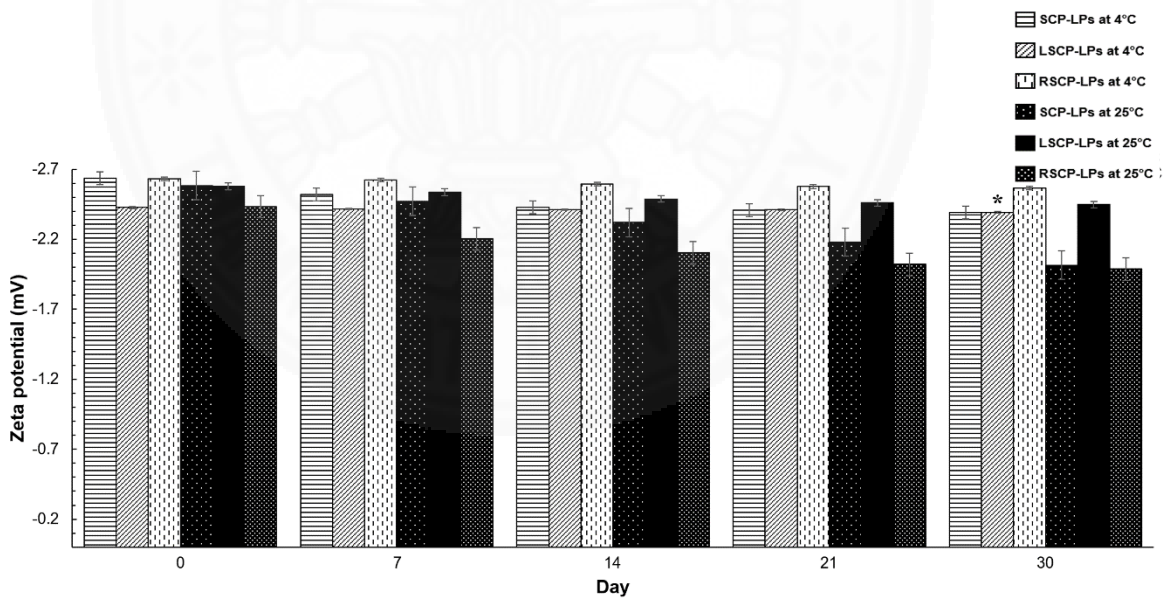
Figure 4.8 Zeta potential of SCP-LPs, LSCP-LPs, and RSCP-LPs at day 0, day 7, day 14, day 21, and day 30 respectively (*n*= 3; Mean±SD) *insignificantly different from day 0 (p-value <0.05).
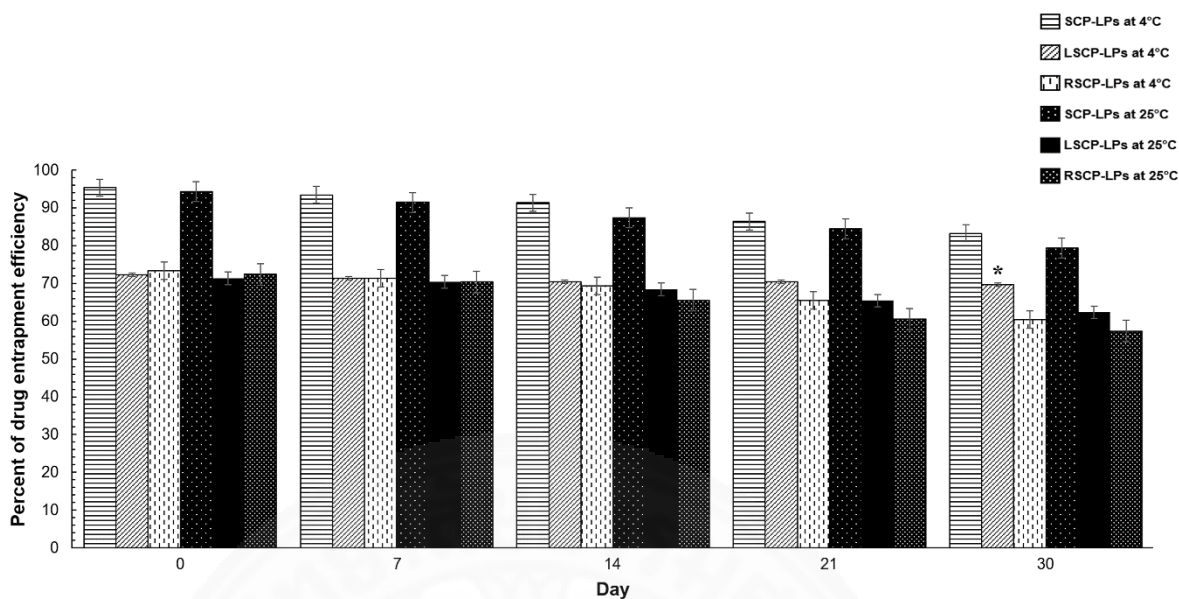
Figure 4.9 Percent of drug entrapment efficiency of SCP-LPs, LSCP-LPs, and RSCP-LPs at day 0, day 7, day 14, day 21, and day 30 respectively (n= 3; Mean±SD) *insignificantly different from day 0 (p-value <0.05).

4.8 *In Vitro* Drug Release Study of LSCP-LPs

Figure 4.10 in **(a)** and **(b)** demonstrated *in vitro* drug release profile of LSCP-LPs redispersed in sterile water. The profile showed that SCP was released from the liposomes around 72% by 8 hours. The obtained drug release profile exhibited biphasic release patterns included initial burst release phase and sustained release phase (Figure 4.10 in **(b)**: (1) and (2)). However, an optimum mathematical model for *in vitro* drug release profile after burst release (Figure 4.10 in **(b)**: (2)) was best fitted with Higuchi's model (Singhvi et al., 2011; Yin et al., 2014) with R-squared value equaled 0.9366 (Figure 4.10 in **(a)**).

This finding could be explained that SCP deposit on LSCP-LPs surface was released immediately after being dispersed in vehicle. After that, the aqueous phase diffused into liposomal structure (matrix of lipid bilayer), SCP embedding in the lipid bilayer were released slowly the receiving media leading to sustained release phase.

Generally, many previous studies revealed that the liposomal drug delivery system could encapsulate and deliver various therapeutic agents. Moreover, it could provide sustained drug release which would increase bioavailability of them. Tabandeh (2013) reported that the *in vitro* drug release pattern of α-tocopherol-loaded liposomes was fitted in zero-order kinetics and found Higuchi's model for minor contribution. These phenomena indicated that their liposomes could generate sustained release property of α-tocopherol. In addition, α-tocopherol-loaded liposomes had higher efficiency to protected the skin from ultraviolet light and free-radical agents when comparing with single anti-oxidative agents. Furthermore, α-tocopherol-loaded liposomes had higher penetration in layer of stratum corneum of the skin when comparing with single anti-oxidative agents.
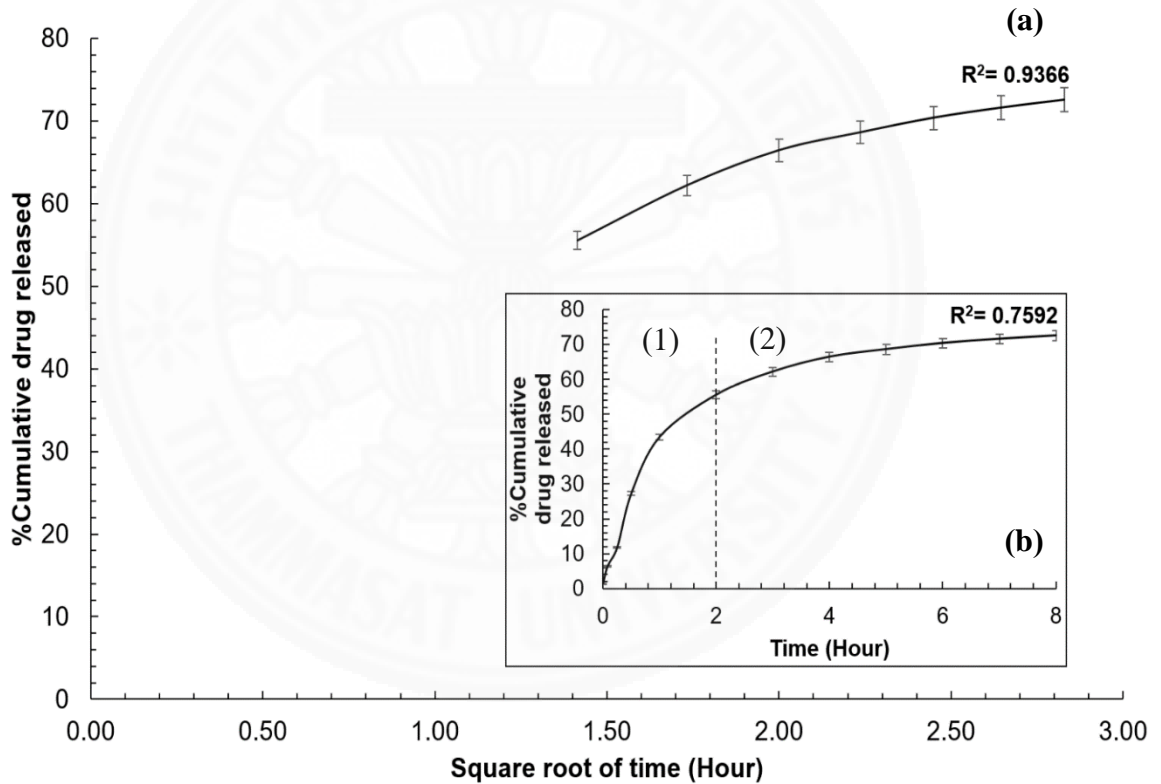
Figure 4.10 *In vitro* drug release patterns of LSCP-LPs: **(a)** Higuchi's model and **(b)** zero-order kinetic model (*n*=3; Mean±SD).

4.9 *In Vitro* Eye Irritation Test of LSCP-LPs

The *in vitro* eye irritation test of LSCP-LPs was performed by using 2 concentration of LSCP-LPs dispersed in media for SIRC cells i.e. 0.05% and 5%. Table 4.5 revealed that percent of cell viability (%CV) of SIRC cells incubated with either 0.05% and 5% of LSCP-LPs were more than 70%. Consequently, the obtained scores for each concentration were one. This implied that LSCP-LPs did not cause irritation in SIRC cells. This is due to the fact that the compositions used in LSCP-LPs formulation were generally recognized as safe.

In addition, their compositions were the essential biological substances to regulated and maintained the cell functions. Phospholipids of LSCP-LPs could be utilized in numerous drug delivery systems with several advantages such as high biocompatible material, non-cytotoxicity, and improved bioavailability of the delivered drugs (Li et al., 2015). Cholesterol is an essential composition of cells. It could maintain and balance rigidity organization of the cell membrane. Zhao et al. (2007) reported that the increment of cholesterol concentration in paclitaxel-loaded liposomes could reduce physical instability when comparing to lower cholesterol content formulations. SCP is an active ingredient in LSCP-LPs, it is commonly found in many kinds of cells and is necessary biological substance via mitogenic activity. SCP could regulate several functions of the cell through signaling pathway i.e. cell proliferation, cell differentiation, cell migration, and re-epithelialization.

Moreover, Esquirol et al. (2014) reported that SCP was an essential therapeutic agent as the wound healing enhancer with high potential and safety to use in several clinical problems i.e. surgical injury, gastroesophageal tract ulcer, and corneal abrasion.

Table 4.5 %CV of SIRC cells and score criterion of short time exposure test (STE) for various concentrations of LSCP-LPs (n= 3; Mean±SD).

Formulation	%CV of SIRC cells	STE irritation score	Scores obtained
0.05% LSCP-LPs	96.36±2.58	If CV>70%: scored 1	1
		If CV≤70%: scored 2	
5% LSCP-LPs	92.16±0.44	If CV>70%: scored 0	0
		If CV≤70%: scored 1	
		Total score:	1

4.10 *In Vitro* Cell Proliferation-Promoting Activity Test of LSCP-LPs

The *in vitro* cell proliferation-promoting activity test was performed by using 5% of empty liposomes and 5% LSCP-LPs in media for SIRC cells. Table 4.6 reported that %CV of SIRC cells incubated with these test samples. It was found that LSCP-LPs exhibited higher potential for increase of cell proliferation than that of empty liposomes. This is due to the fact that SCP is an essential mitogenic agent usually found that in epidermal cells, endothelial cells, fibroblast cells, glial cells, and corneal endothelial cells. As described in Topic 2.4, the action of SCP is occurred via signaling pathway from high specificity interaction between of the SCP and the extracellular domain of SCP receptor (signal transducer-activator of transcription: STAT). SCP could activate ligand-induced dimerization of SCP receptors. After that, dimerized cytoplasmic membrane of SCP receptor (intracytoplasmic janus kinase: JAK) were arranged to tyrosine kinase pro-teins and induced transphosphorylation for tyrosine residues in the cytoplasmic domain of SCP receptor. The phosphorylated tyrosine of SCP receptor would stimulate intra-cellular proteins called GRB2 and SOS. Then, GRB2 and SOS would induce increment of glycolysis and protein synthesis. In addition, GRB2 and SOS could stimulate gene transcrip-tion leading to cell proliferation, inhibition of apoptosis, angiogenesis, and cell migration (Hardwicke et al., 2008).

Table 4.6 showed that LSCP-LPs could promote SIRC cells proliferation more than empty liposomes around 8%. This suggested that LSCP-LPs could be used for further *in vivo* study to investigate their activity for treatment of corneal abrasion. However, the optimization concentration of SCP should be determined as well to increase their activity.

Table 4.6 %CV of SIRC cells for 5% empty liposomes and 5% LSCP-LPs (*n*= 3; Mean± SD).

Formulation	%CV of SIRC cells	%Cell proliferation of LSCP-LPs
5% empty liposomes	114.62±4.64	
		8.69
5% LSCP-LPs	124.11±3.78	

CHAPTER 5
CONCLUSIONS AND RECOMMENDATIONS

The results showed that increment of sonication time of SCP-LPs could induce their particle diameter in a range of nanometer with narrow particle size distribution. In addition, increase of sonication time of SCP-LPs could influence higher zeta potential and drug entrapment efficiency when comparing with lower exposure time of the ultrasonic waves.

The effects of solidification and cryoprotectant concentration of LSCP-LPS exhibited that suitable freezing temperature and sucrose concentration of LSCP-LPs could maintain their particle diameter with acceptance particle size distribution. In addition, optimized LSCP-LPs had higher zeta potential and drug entrapment efficiency when comparing with other freezing temperatures and sucrose concentrations. Moreover, the SEM- and TEM photomicrographs of optimized LSCP-LPs exhibited that LSCP-LPs had spherical shape with unilamellar vesicles and disappeared liposomal degradation.

The results of XRD analysis and thermal analysis of LSCP-LPs implied that the chemical interaction of compositions of LSCP-LPs were arranged and transformed into new specific ordered organization with amorphous characteristic. Their results indicated that SCP could incorporate and disperse in lipid bilayer of LSCP-LPs. Moreover, FT-IR spectrum of LSCP-LPs indicated that SCP could substitute their structure into liposomal structure of LSCP-LPs.

In addition, the results of stability evaluation of SCP-LPs, LSCP-LPs and RSCP-LPs revealed that LSCP-LPs under storage temperature at 4°C had higher physico-chemical stability and did not show significantly difference when comparing with their initial day.

The results of *in vitro* drug release study of LSCP-LPs demonstrated that LSCP-LPs had biphasic release patterns included initial burst release phase and sustained release phase. However, an optimal mathematical model for *in vitro* drug release profile of LSCP-LPs was best fitted in Higuchi's model.

The results of *in vitro* eye irritation test of LSCP-LPs exhibited that LSCP-LPs did not show irritation effects in SIRC cells. Moreover, the results of *in vitro* cell proliferation-promoting activity test of LSCP-LPs revealed that LSCP-LPs had higher potential to stimulate cell proliferation activity of SIRC cells when comparing with empty liposomes. Therefore, the results of pharmacological activities of LSCP-LPs demonstrated that LSCP-LPs had high safety and efficiency to utilize in ophthalmic application.

However, the optimized LSCP-LPs was statistically significance of their drug entrapment efficiency when comparing with SCP-LPs. Therefore, further studies for optimization of production process and formulation composition of LSCP-LPs are necessary for improvement of their physicochemical properties and pharmacological activities.
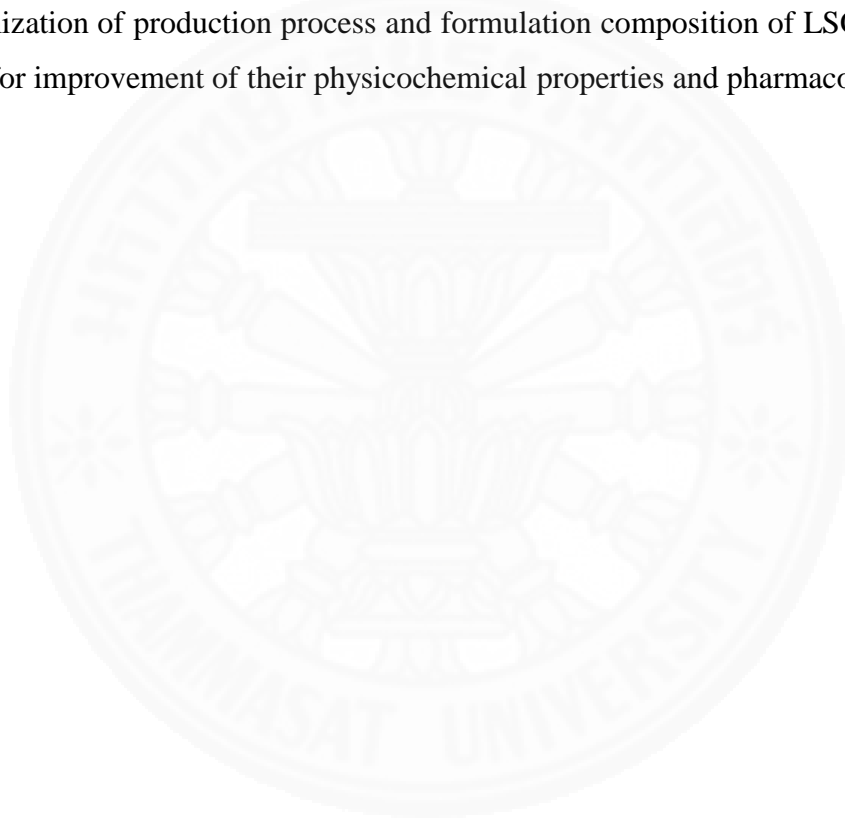
REFERENCES

Abdelbary G. Ocular ciprofloxacin hydrochloride muco-adhesive chitosan-coated liposomes. Journal of Pharmaceutical Development and Technology. 2011;16(1):44-56.

Akbarzadeh A, Rezaei-Sadabady R, Davaran S, Joo SW, Zarghami N, Hanifehpour Y, et al. Liposome: classification, preparation, and applications. Nanoscale Research Letters. 2013;8(1):102.

Alipour M, Halwani M, Omri A, Suntres ZE. Antimicrobial effectiveness of liposomal polymyxin B against resistant gram-negative bacterial strains. International Journal of Pharmaceutics. 2008;355(1-2):293-8.

Alves JB, Ferreira CL, Martins AF, Silva GAB, Alves GD, Paulino TP, et al. Local delivery of EGF-liposome mediated bone modeling in orthodontic tooth movement by increasing RANKL expression. Journal of Life Sciences. 2009;85(19-20):693-9.

Aso Y, Yoshioka S. Effect of freezing rate on physical stability of lyophilized cationic liposomes. Chemical and Pharmaceutical Bulletin. 2005;53(3):301-4.

Barrientos S, Brem H, Stojadinovic O, Tomic-Canic M. Clinical application of growth factors and cytokines in wound healing. Journal of The Wound Healing Society and the European Tissue Repair Society. 2014;22(5):569-78.

Celebi N, Turkyilmaz A, Gonul B, Ozogul C. Effects of epidermal growth factor microemulsion formulation on the healing of stress-induced gastric ulcers in rats. Journal of The Controlled Release Society. 2002;83(2):197-210.

Chang W-K, Tai Y-J, Chiang C-H, Hu C-S, Hong P-D, Yeh M-K. The comparison of protein-entrapped liposomes and lipoparticles: preparation, characterization, and efficacy of cellular uptake. International Journal of Nanomedicine. 2011;6: 2403-17.

Charnvanich D, Vardhanabhuti N, Kulvanich P. Effect of cholesterol on the properties of spray-dried lysozyme-loaded liposomal powders. Journal of Pharmaceutical Sciences and Technology. 2010;11(2):832-42.

Chaudhury A, Das S, Lee RFS, Tan K-B, Ng W-K, Tan RBH, et al. Lyophilization of cholesterol-free PEGylated liposomes and its impact on drug loading by passive equilibration. International Journal of Pharmaceutics. 2012;430(1-2):167-75.

Chen C, Han D, Cai C, Tang X. An overview of liposome lyophilization and its future potential. Journal of The Controlled Release Society. 2010;142(3):299-311.

Chime SA, Umeyor EC, Onyishi VI, Onunkwo GC, Attama AA. Analgesic and micromeritic evaluations of SRMS-based oral liposures of diclofenac potassium. Indian Journal of Pharmaceutical Sciences. 2013;75(3):302-9.

Chithrani DB, Dunne M, Stewart J, Allen C, Jaffray DA. Cellular uptake and transport of gold nanoparticles incorporated in a liposomal carrier. Journal of Nanomedicine. 2010;6(1):161-9.

Değim Z. Use of microparticulate systems to accelerate skin wound healing. Journal of Drug Targeting. 2008;16(6):437-48.

Del Amo EM, Urtti A. Current and future ophthalmic drug delivery systems. Letter of Drug Discovery Today. 2008;13(3-4):135-43.

El-Nesr OH, Yahiya SA, El-Gazayerly ON. Effect of formulation design and freeze-drying on properties of fluconazole multilamellar liposomes. Saudi Pharmaceutical Journal. 2010;18(4):217-24.

Esquirol Caussa J, Herrero Vila E. Epidermal growth factor: innovation and safety. Journal of Medicina Clinica. 2015;145(7):305-12.

Fujisawa T, Miyai H, Hironaka K, Tsukamoto T, Tahara K, Tozuka Y, et al. Liposomal diclofenac eye drop formulations targeting the retina: formulation stability improvement using surface modification of liposomes. International Journal of Pharmaceutics. 2012;436(1-2):564-7.

Gaudana R, Ananthula HK, Parenky A, Mitra AK. Ocular drug delivery. Journal of Pharmaceutical Sciences and Technology. 2010;12(3):348-60.

Ghanbarzadeh S, Valizadeh H, Zakeri-Milani P. The effects of lyophilization on the physicochemical stability of sirolimus liposomes. Advanced Pharmaceutical Bulletin. 2013;3(1):25-9.

Gil ES, Panilaitis B, Bellas E, Kaplan DL. Functionalized silk biomaterials for wound healing. Journal of Advanced Healthcare Materials. 2013;2(1):206-17.

Gregoriadis G. Liposomes in drug delivery: how it all happened. Journal of Pharmaceutics. 2016;8(2):19.

Han H-K, Shin H-J, Ha DH. Improved oral bioavailability of alendronate via the mucoadhesive liposomal delivery system. European Journal of Pharmaceutical Sciences. 2012;46(5):500-7.

Hanaor D, Michelazzi M, Leonelli C, Sorrell CC. The effects of carboxylic acids on the aqueous dispersion and electrophoretic deposition of ZrO_2. Journal of The Euro pean Ceramic Society. 2012;32(1):235-44.

Hardwicke J, Schmaljohann D, Boyce D, Thomas D. Epidermal growth factor therapy and wound healing in past, present and future perspectives. Journal of The Royal Colleges of Surgeons of Edinburgh and Ireland. 2008;6(3):172-7.

Hathout RM, Mansour S, Mortada ND, Guinedi AS. Liposomes as an ocular delivery system for acetazolamide: *in vitro* and *in vivo* studies. Journal of Pharmaceutical Sciences and Technology. 2007;8(1):1.

Himanshu A, Sitasharan P, Singhai AK. Liposomes as drug carriers. International Journal of Pharmaceutical and Life Sciences. 2011;2(7):945-51.

Immordino ML, Dosio F, Cattel L. Stealth liposomes: review of the basic science, rationale, and clinical applications, existing and potential. International Journal of Nanomedicine. 2006;1(3):297.

Jangle RD, Thorat BN. Effect of freeze-thawing study on curcumin liposome for obtaining better freeze-dried product. Journal of Drying Technology. 2013;31(9):966-74.

Kasper JC, Friess W. The freezing step in lyophilization: physicochemical fundamentals, freezing methods and consequences on process performance and quality attributes of biopharmaceuticals. European Journal of Pharmaceutics and Biopharmaceutics. 2011;78(2):248-63.

Kataria S, Sandhu P, Bilandi A, Akanksha M, Kapoor B, Seth GL, Bihani SD. Stealth liposomes: a review. International Journal of Research in Ayurveda and Pharmacy. 2011;2(5):1534-38.

Klenkler B, Sheardown H, Jones L. Growth factors in the tear film: role in tissue maintenance, wound healing, and ocular pathology. Journal of The Ocular Surface. 2007;5(3):228-39.

Konkimalla VB, McCubrey JA, Efferth T. The role of downstream signaling pathways of the epidermal growth factor receptor for artesunate activity in cancer cells. Journal of Current Cancer Drug Targets. 2009;9(1):72-80.

Li J, Wang X, Zhang T, Wang C, Huang Z, Luo X, et al. A review on phospholipids and their main applications in drug delivery systems. Asian Journal of Pharmaceutical Sciences. 2015;10(2):81-98.

Li N, Zhuang C, Wang M, Sun X, Nie S, Pan W. Liposome coated with low molecular weight chitosan and its potential use in ocular drug delivery. International Journal of Pharmaceutics. 2009;379(1):131-8.

Liu M, Chen L, Zhao Y, Gan L, Zhu D, Xiong W, et al. Preparation, characterization and properties of liposome-loaded polycaprolactone microspheres as a drug delivery system. Journal of Physicochemical and Engineering Aspects. 2012;395:131-6.

Lurje G, Lenz HJ. EGFR signaling and drug discovery. Journal of Oncology. 2009;77(6):400-10.

Marquez L, de Abreu FAM, Ferreira CL, Alves GD, Miziara MN, Alves JB. Enhanced bone healing of rat tooth sockets after administration of epidermal growth factor carried by liposome. Journal of Injury. 2013;44(4):558-64.

Martinez-Santamaria L, Conti CJ, Llames S, Garcia E, Retamosa L, Holguin A, et al. The regenerative potential of fibroblasts in a new diabetes-induced delayed humanized wound healing model. Journal of Dermatology. 2013;22(3):195-201.

Menke NB, Ward KR, Witten TM, Bonchev DG, Diegelmann RF. Impaired wound healing. Journal of Dermatology. 2007;25(1):19-25.

Ming-Ren Toha GNCC. Liposomes as sterile preparations and limitations of sterilization techniques in liposomal manufacturing. Asian Journal of Pharmaceutical Sciences. 2013;8(2):88-95.

Miyazaki Y, Ogihara K, Yakou S, Nagai T, Takayama K. *In vitro* and *in vivo* evaluation of muco-adhesive microspheres consisting of dextran derivatives and cellulose acetate butyrate. International Journal of Pharmaceutics. 2003;258(1-2):21-9.

Moen MD, Lyseng-Williamson KA, Scott LJ. Liposomal amphotericin B: a review of its use as empirical therapy in febrile neutropenia and in the treatment of invasive fungal infections. Drugs Bulletin. 2009;69(3):361-92.

Mohan VK. Recombinant human epidermal growth factor (REGEN-D 150): effect on healing of diabetic foot ulcers. Journal of Diabetes Research and Clinical Practice. 2007;78(3):405-11.

Muppidi K, Pumerantz AS, Wang J, Betageri G. Development and stability studies of novel liposomal vancomycin formulations. Pharmaceutics Journal of International Scholarly Research Notices. 2012;2012:8.

Nireesha G. R, Divya L, Sowmya C. Lyophilization: a review. International Journal of Novel Trends in Pharmaceutical Sciences. 2013;3(4):87-98.

Ohshima H, Miyagishima A, Kurita T, Makino Y, Iwao Y, Sonobe T, et al. Freeze-dried nifedipine-lipid nanoparticles with long-term nano-dispersion stability after reconstitution. International Journal of Pharmaceutics. 2009;377(1-2):180-4.

Patel A, Cholkar K, Agrahari V, Mitra AK. Ocular drug delivery systems: an overview. World Journal of Pharmacology. 2013;2(2):47-64.

Payton NM, Wempe MF, Xu Y, Anchordoquy TJ. Long-term storage of lyophilized liposomal formulations. Journal of Pharmaceutical Sciences. 2014;103(12): 3869-78.

Sacchetti M, Lambiase A. Diagnosis and management of neurotrophic keratitis. Journal of Clinical Ophthalmology. 2014;8:571-9.

Schwendener RA. Liposomes as vaccine delivery systems: a review of the recent advances. Journal of Therapeutic Advances in Vaccines. 2014;2(6):159-82.

Seetharamu N, Kim E, Hochster H, Martin F, Muggia F. Phase II study of liposomal cisplatin (SPI-77) in platinum-sensitive recurrences of ovarian cancer. Journal of Anticancer Research. 2010;30(2):541-5.

Sezgin-Bayindir Z, Yuksel N. Investigation of formulation variables and excipient interaction on the production of niosomes. Asian Journal of Pharmaceutical Sciences. 2012;13(3):826-35.

Shashi K, Satinder K, Bharat P. A complete review on liposome. International Research Journal of Pharmacy. 2012;3(7):10-6.

Sundar S, Chakravarty J. Liposomal amphotericin B and leishmaniasis: dose and response. Journal of Global Infectious Diseases. 2010;2(2):159-66.

Tabandeh H, Mortazavi SA. An investigation into some effective factors on encapsulation efficiency of alpha-tocopherol in MLVs and the release profile from the corresponding liposomal gel. Iranian Journal of Pharmaceutical Research. 2013;12: 21-30.

Tanigawa T, Ahluwalia A, Watanabe T, Arakawa T, Tarnawski AS. Nerve growth factor injected into the gastric ulcer base incorporates into endothelial, neuronal, glial and epithelial cells: implications for angiogenesis, mucosal regeneration and ulcer healing. Journal of Physiology and Pharmacology. 2015;66(4):617-21.

Throm AM, Liu WC, Lock CH, Billiar KL. Development of a cell-derived matrix: effects of epidermal growth factor in chemically defined culture. Journal of Biomedical Materials Research. 2010;92(2):533-41.

Vural I, Sarisozen C, Olmez SS. Chitosan coated furosemide liposomes for improved bioavailability. Journal of Biomedical Nanotechnology. 2011;7(3):426-30.

Wang D, Kong L, Wang J, He X, Li X, Xiao Y. Polymyxin E sulfate-loaded liposome for intravenous use: preparation, lyophilization, and toxicity assessment. Journal of Pharmaceutical Science and Technology. 2009;63(2):159-67.

Wang H, Zhao P, Liang X, Gong X, Song T, Niu R, et al. Folate-PEG coated cationic modified chitosan-cholesterol liposomes for tumor-targeted drug delivery. Journal of Biomaterials. 2010;31(14):4129-38.

Wipperman JL, Dorsch JN. Evaluation and management of corneal abrasions. American Family Physician Journal. 2013;87(2):114-20.

Woodbury DJ, Richardson ES, Grigg AW, Welling RD, Knudson BH. Reducing liposome size with ultrasound: bimodal size distributions. Journal of Liposome Research. 2006;16(1):57-80.

Yang CH, Wu PC, Huang YB, Tsai YH. A new approach for determining the stability of recombinant human epidermal growth factor by thermal fourier transform infrared microspectroscopy. Journal of Biomolecular Structure and Dynamics. 2004;22(1): 101-10.

Yin F, Guo S, Gan Y, Zhang X. Preparation of redispersible liposomal dry powder using an ultrasonic spray freeze-drying technique for transdermal delivery of human epithelial growth factor. International Journal of Nanomedicine. 2014;9:1665-76.

Yokota D, Moraes M, Pinho SC. Characterization of lyophilized liposomes produced with non-purified soy lecithin: a case study of casein hydrolysate microencapsulation. Brazilian Journal of Chemical Engineering. 2012;29:325-35.

Yoshida P, Yokota D, Foglio M, Rodrigues RF, Pinho S. Liposomes incorporating essential oil of Brazilian cherry: characterization of aqueous dispersions and lyophilized formulations. Journal of Microencapsulation. 2010;27(5):416-25.

Zhang F, Yang H, Pan Z, Wang Z, Wolosin JM, Gjorstrup P, et al. Dependence of resolving induced increases in corneal epithelial cell migration on EGF receptor transactivation. Journal of Investigative Ophthalmology and Visual Science. 2010;51(11): 5601-9.

Zhao L, Feng S-S, Kocherginsky N, Kostetski I. DSC and EPR investigations on effects of cholesterol component on molecular interactions between paclitaxel and phospholipid within lipid bilayer membrane. International Journal of Pharmaceutics. 2007;338(1-2):258-66.

APPENDICES

APPENDIX A

CALIBRATION CURVE DETAILS OF THE SCP DETERMINATION
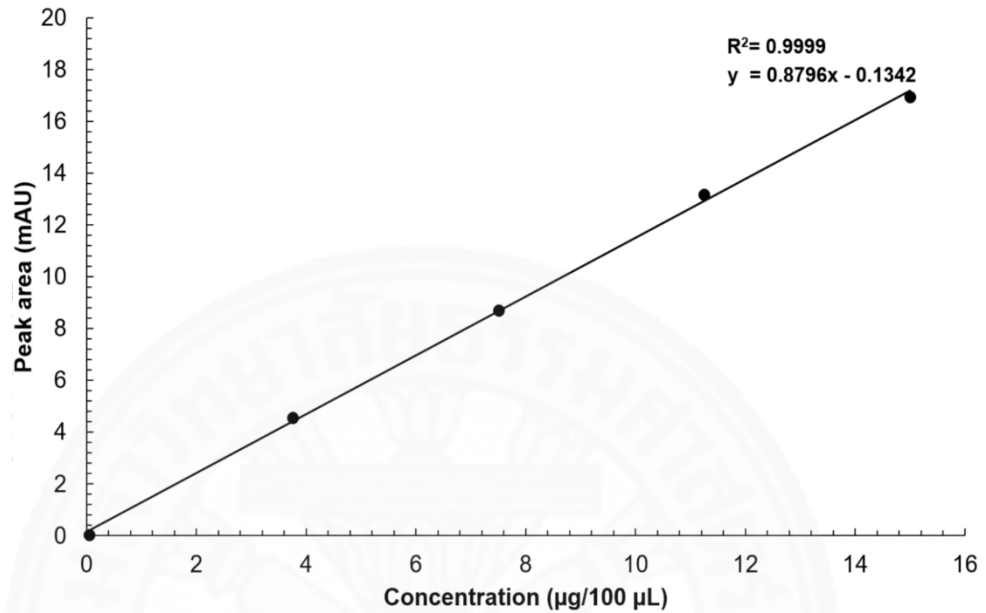
Figure A1 Calibration curve of the SCP determination.

Table A1 Details of the calibration curve of SCP determination.

Standard of SCP	Peak area (mAU)	Concentration (µg/100 µL)
0.3% SCP	0.0259	0.0452
25% SCP	4.5628	3.7516
50% SCP	8.7113	7.5429
75% SCP	13.1859	11.2531
100% SCP	16.9593	15.0714

APPENDIX B

RESULTS AND STATISTICAL ANALYSIS DATA OF SCP-LPs

Table B1 Particle size of SCP-LPs with various sonication time intervals (n= 3; Mean±SD).

Sonication time (minute)	Particle size (nm)
0	88.59±0.12
1	87.87±0.03
3	84.84±0.07
5	81.12±0.09

Table B2 Statistical analysis data of particle size of SCP-LPs with various sonication time intervals.

Sonication time (minute)		p-value	Mean Square	F-value
0	1	<0.05	34.77	4.68E+003
	3	<0.05		
	5	<0.05		
1	0	<0.05		
	3	<0.05		
	5	<0.05		
3	0	<0.05		
	1	<0.05		
	5	<0.05		
5	0	<0.05		
	1	<0.05		
	3	<0.05		

Table B3 PDI of SCP-LPs with various sonication time intervals ($n= 3$; Mean±SD).

Sonication time (minute)	PDI
0	0.23±0.00
1	0.23±0.00
3	0.23±0.00
5	0.22±0.00

Table B4 Statistical analysis data of PDI of SCP-LPs with various sonication time intervals.

Sonication time (minute)		p-value	Mean Square	F-value
0	1	0.99	0.00	0.27
	3	0.98		
	5	0.93		
1	0	0.99		
	3	0.93		
	5	0.85		
3	0	0.98		
	1	0.93		
	5	0.99		
5	0	0.92		
	1	0.85		
	3	0.99		

Table B5 Zeta potential of SCP-LPs with various sonication time intervals (n= 3; Mean± SD).

Sonication time (minute)	Zeta potential (mV)
0	-1.13±0.14
1	-2.27±0.07
3	-2.46±0.02
5	-2.95±0.04

Table B6 Statistical analysis data of zeta potential of SCP-LPs with various sonication time intervals.

Sonication time (minute)		p-value	Mean Square	F-value
0	1	<0.05	1.77	2.99E+003
	3	<0.05		
	5	<0.05		
1	0	<0.05		
	3	<0.05		
	5	<0.05		
3	0	<0.05		
	1	<0.05		
	5	<0.05		
5	0	<0.05		
	1	<0.05		
	3	<0.05		

Table B7 Drug entrapment efficiency of SCP-LPs with various sonication time intervals ($n= 3$; Mean±SD).

Sonication time (minute)	Drug entrapment efficiency (%)
0	23.54±0.93
1	35.45±1.12
3	93.69±1.04
5	97.56±0.85

Table B8 Statistical analysis data of drug entrapment efficiency of SCP-LPs with various sonication time intervals.

Sonication time (minute)		p-value	Mean Square	F-value
0	1	<0.05	4.44E+003	9.40E+004
	3	<0.05		
	5	<0.05		
1	0	<0.05		
	3	<0.05		
	5	<0.05		
3	0	<0.05		
	1	<0.05		
	5	<0.05		
5	0	<0.05		
	1	<0.05		
	3	<0.05		

APPENDIX C

RESULTS AND STATISTICAL ANALYSIS DATA OF LSCP-LPs

Table C1 Particle size of LSCP-LPs with various freezing temperatures (n= 3; Mean±SD).

Freezing temperature (°C)	Particle size (nm)
SCP-LPs	81.12±0.09
-20	89.54±0.21
-40	81.56±0.13
-80	108.93±0.15

Table C2 Statistical analysis data of particle size of LSCP-LPs with various freezing temperatures

Freezing temperature (°C)		p-value	Mean Square	F-value
SCP-LPs	-20	<0.05	508.50	1.64E+004
	-40	0.06		
	-80	<0.05		
-20	SCP-LPs	<0.05		
	-40	<0.05		
	-80	<0.05		
-40	SCP-LPs	0.06		
	-20	<0.05		
	-80	<0.05		
-80	SCP-LPs	<0.05		
	-20	<0.05		
	-40	<0.05		

Table C3 PDI of LSCP-LPs with various freezing temperatures (*n*= 3; Mean±SD).

Freezing temperature (°C)	PDI
SCP-LPs	0.22±0.00
-20	0.28±0.00
-40	0.23±0.00
-80	0.43±0.00

Table C4 Statistical analysis data of PDI of LSCP-LPs with various freezing temperatures.

Freezing temperature (°C)		*p*-value	Mean Square	F-value
SCP-LPs	-20	<0.05	0.03	1.46E+004
	-40	0.07		
	-80	<0.05		
-20	SCP-LPs	<0.05		
	-40	<0.05		
	-80	<0.05		
-40	SCP-LPs	0.07		
	-20	<0.05		
	-80	<0.05		
-80	SCP-LPs	<0.05		
	-20	<0.05		
	-40	<0.05		

Table C5 Zeta potential of LSCP-LPs with various freezing temperatures (n= 3; Mean± SD).

Freezing temperature (°C)	Zeta potential (mV)
SCP-LPs	-2.95±0.04
-20	-2.03±0.02
-40	-2.90±0.03
-80	-1.94±0.03

Table C6 Statistical analysis data of zeta potential of LSCP-LPs with various freezing temperatures.

Freezing temperature (°C)		p-value	Mean Square	F-value
SCP-LPs	-20	<0.05	0.88	1.11E+003
	-40	0.21		
	-80	<0.05		
-20	SCP-LPs	<0.05		
	-40	<0.05		
	-80	0.02		
-40	SCP-LPs	0.21		
	-20	<0.05		
	-80	<0.05		
-80	SCP-LPs	<0.05		
	-20	0.02		
	-40	<0.05		

Table C7 Drug entrapment efficiency of LSCP-LPs with various freezing temperatures (*n*= 3; Mean±SD).

Freezing temperature (°C)	Drug entrapment efficiency (%)
SCP-LPs	97.56±0.85
-20	45.54±0.38
-40	73.28±0.93
-80	65.46±0.22

Table C8 Statistical analysis data of drug entrapment efficiency of LSCP-LPs with various freezing temperatures.

Freezing temperature (°C)		*p*-value	Mean Square	F-value
SCP-LPs	-20	<0.05	1.38E+003	1.11E+003
	-40	<0.05		
	-80	<0.05		
-20	SCP-LPs	<0.05		
	-40	<0.05		
	-80	<0.05		
-40	SCP-LPs	<0.05		
	-20	<0.05		
	-80	<0.05		
-80	SCP-LPs	<0.05		
	-20	<0.05		
	-40	<0.05		

Table C9 Particle size of LSCP-LPs with various cryoprotectant concentrations ($n= 3$; Mean±SD).

Cryoprotectant concentration (Molar ratio)	Particle size (nm)
SCP-LPs	81.12±0.09
1:0	1829.00±2.00
1:1	92.91±0.06
1:3	85.50±0.29
1:5	81.56±0.13

Table C10 Statistical analysis data of particle size of LSCP-LPs with cryoprotectant concentrations.

Cryoprotectant concentration (Molar ratio)		p-value	Mean Square	F-value
SCP-LPs	1:0	<0.05	1.82E+006	2.20E+006
	1:1	<0.05		
	1:3	<0.05		
	1:5	0.97		
1:0	SCP-LPs	<0.05		
	1:1	<0.05		
	1:3	<0.05		
	1:5	<0.05		
1:1	SCP-LPs	<0.05		
	1:0	<0.05		
	1:3	<0.05		
	1:5	<0.05		

Table C10 Statistical analysis data of particle size of LSCP-LPs with cryoprotectant concentrations. (Cont.)

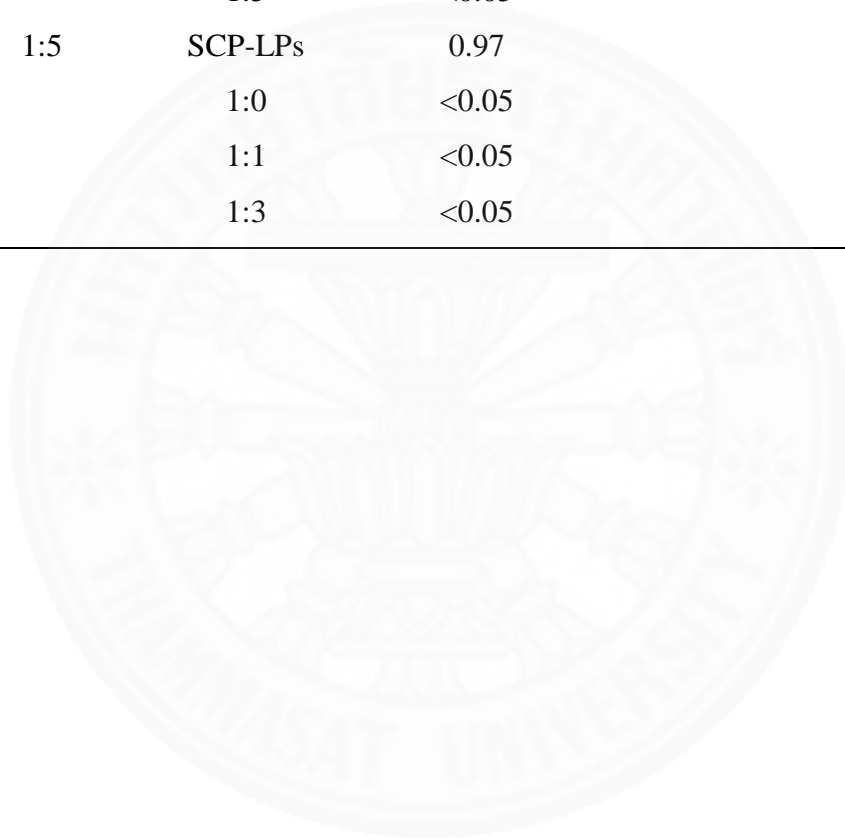| Cryoprotectant concentration (Molar ratio)		p-value	Mean Square	F-value
1:3	SCP-LPs	<0.05		
	1:0	<0.05		
	1:1	<0.05		
	1:5	<0.05		
1:5	SCP-LPs	0.97		
	1:0	<0.05		
	1:1	<0.05		
	1:3	<0.05		

Table C11 PDI of LSCP-LPs with various cryoprotectant concentrations (*n*= 3; Mean±SD).

Cryoprotectant concentration (Molar ratio)	PDI
SCP-LPs	0.22±0.00
1:0	Not detected (1.00±0.00)
1:1	0.39±0.00
1:3	0.27±0.00
1:5	0.23±0.00

Table C12 Statistical analysis data of PDI of LSCP-LPs with cryoprotectant concentrations.

Cryoprotectant concentration (Molar ratio)		*p*-value	Mean Square	F-value
SCP-LPs	1:0	<0.05	0.32	1.48E+005
	1:1	<0.05		
	1:3	<0.05		
	1:5	0.11		
1:0	SCP-LPs	<0.05		
	1:1	<0.05		
	1:3	<0.05		
	1:5	<0.05		
1:1	SCP-LPs	<0.05		
	1:0	<0.05		
	1:3	<0.05		
	1:5	<0.05		

Table C12 Statistical analysis data of PDI of LSCP-LPs with cryoprotectant concentrations. (Cont.)

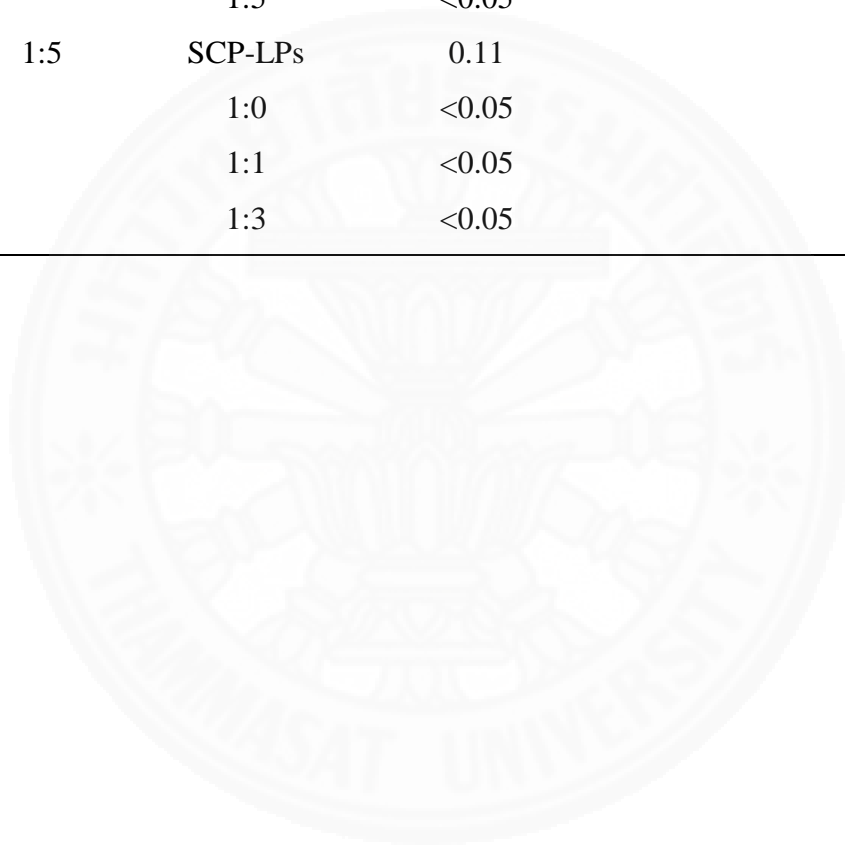| Cryoprotectant concentration (Molar ratio)		p-value	Mean Square	F-value
1:3	SCP-LPs	<0.05		
	1:0	<0.05		
	1:1	<0.05		
	1:5	<0.05		
1:5	SCP-LPs	0.11		
	1:0	<0.05		
	1:1	<0.05		
	1:3	<0.05		

Table C13 Zeta potential of LSCP-LPs with various cryoprotectant concentrations (n= 3; Mean±SD).

Cryoprotectant concentration (Molar ratio)	Zeta potential (mV)
SCP-LPs	-2.95±0.04
1:0	-1.95±0.03
1:1	-2.26±0.04
1:3	-2.38±0.03
1:5	-2.90±0.03

Table C14 Statistical analysis data of zeta potential of LSCP-LPs with cryoprotectant concentrations.

Cryoprotectant concentration (Molar ratio)		p-value	Mean Square	F-value
SCP-LPs	1:0	<0.05	0.55	466.31
	1:1	<0.05		
	1:3	<0.05		
	1:5	0.43		
1:0	SCP-LPs	<0.05		
	1:1	<0.05		
	1:3	<0.05		
	1:5	<0.05		
1:1	SCP-LPs	<0.05		
	1:0	<0.05		
	1:3	0.01		
	1:5	<0.05		

Table C14 Statistical analysis data of zeta potential of LSCP-LPs with cryoprotectant concentrations. (Cont.)

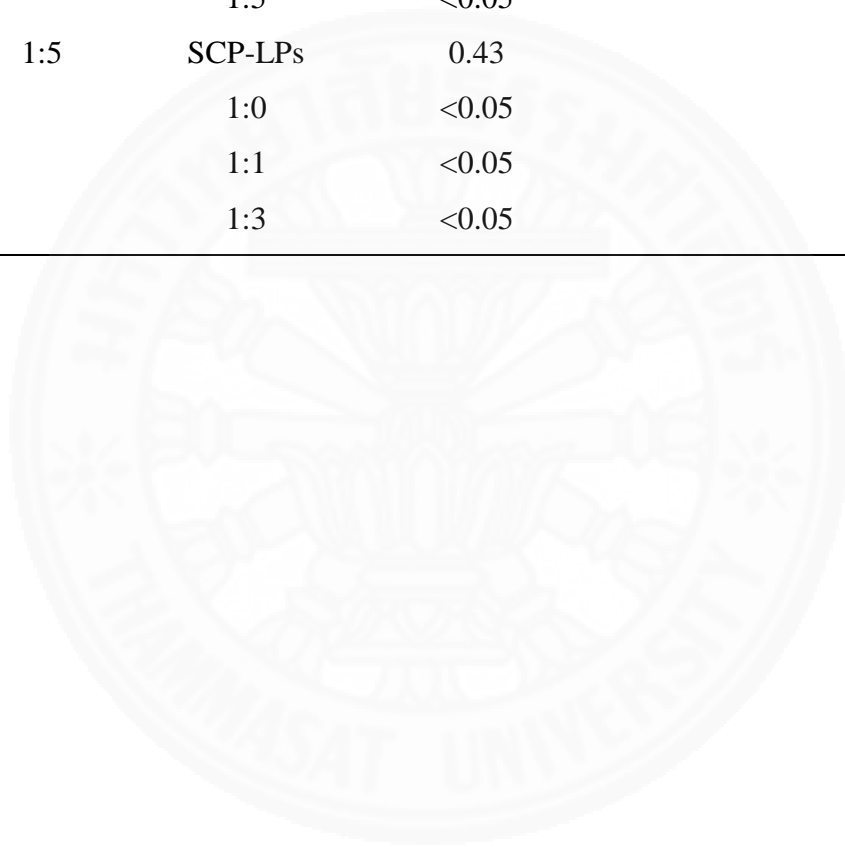| Cryoprotectant concentration (Molar ratio)		p-value	Mean Square	F-value
1:3	SCP-LPs	<0.05		
	1:0	<0.05		
	1:1	0.01		
	1:5	<0.05		
1:5	SCP-LPs	0.43		
	1:0	<0.05		
	1:1	<0.05		
	1:3	<0.05		

Table C15 Drug entrapment efficiency of LSCP-LPs with various cryoprotectant concentrations (n= 3; Mean±SD).

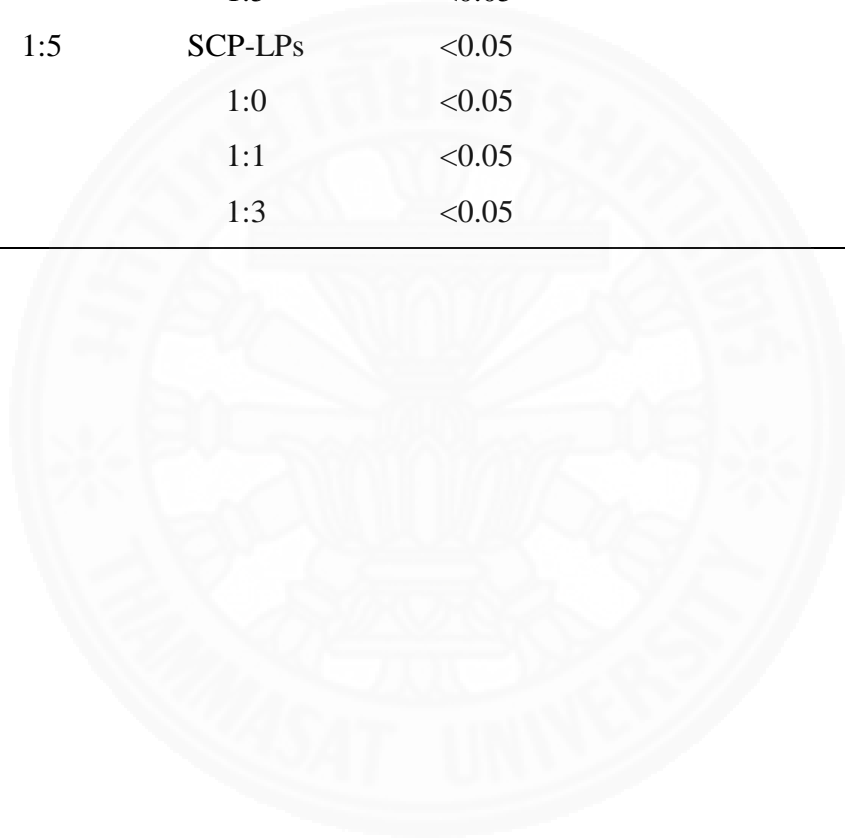| Cryoprotectant concentration (Molar ratio)	Drug entrapment efficiency (%)
SCP-LPs	97.56±0.85
1:0	31.63±0.47
1:1	32.67±0.42
1:3	56.22±0.36
1:5	73.28±0.93

Table C16 Statistical analysis data of drug entrapment efficiency of LSCP-LPs with cryoprotectant concentrations.

Cryoprotectant concentration (Molar ratio)		p-value	Mean Square	F-value
SCP-LPs	1:0	<0.05	2.34E+003	1.91E+004
	1:1	<0.05		
	1:3	<0.05		
	1:5	<0.05		
1:0	SCP-LPs	<0.05		
	1:1	0.03		
	1:3	<0.05		
	1:5	<0.05		
1:1	SCP-LPs	<0.05		
	1:0	0.03		
	1:3	<0.05		
	1:5	<0.05		

Table C16 Statistical analysis data of drug entrapment efficiency of LSCP-LPs with cryo-
protectant concentrations. (Cont.)

Cryoprotectant concentration (Molar ratio)		p-value	Mean Square	F-value
1:3	SCP-LPs	<0.05		
	1:0	<0.05		
	1:1	<0.05		
	1:5	<0.05		
1:5	SCP-LPs	<0.05		
	1:0	<0.05		
	1:1	<0.05		
	1:3	<0.05		

APPENDIX D
X-RAY POWDER DIFFRACTION ANALYSIS DETAILS OF
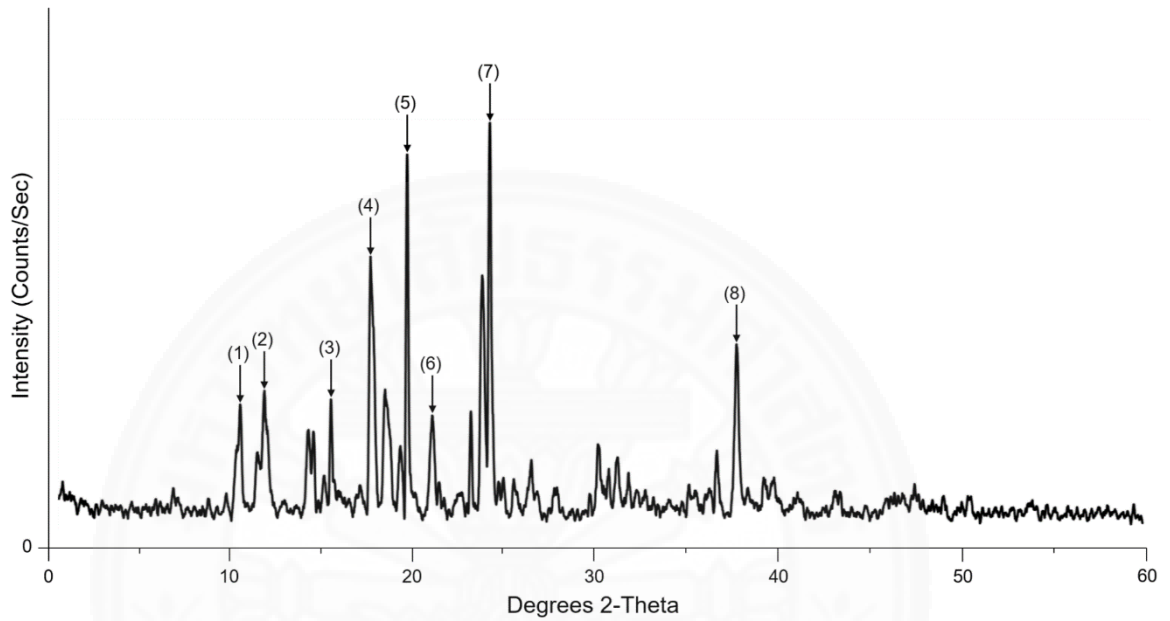# BULK MATERIALS AND LSCP-LPs

Figure D1 X-ray powder diffraction pattern of physical mixture.

Table D1 Details of X-ray powder diffraction analysis of physical mixture.

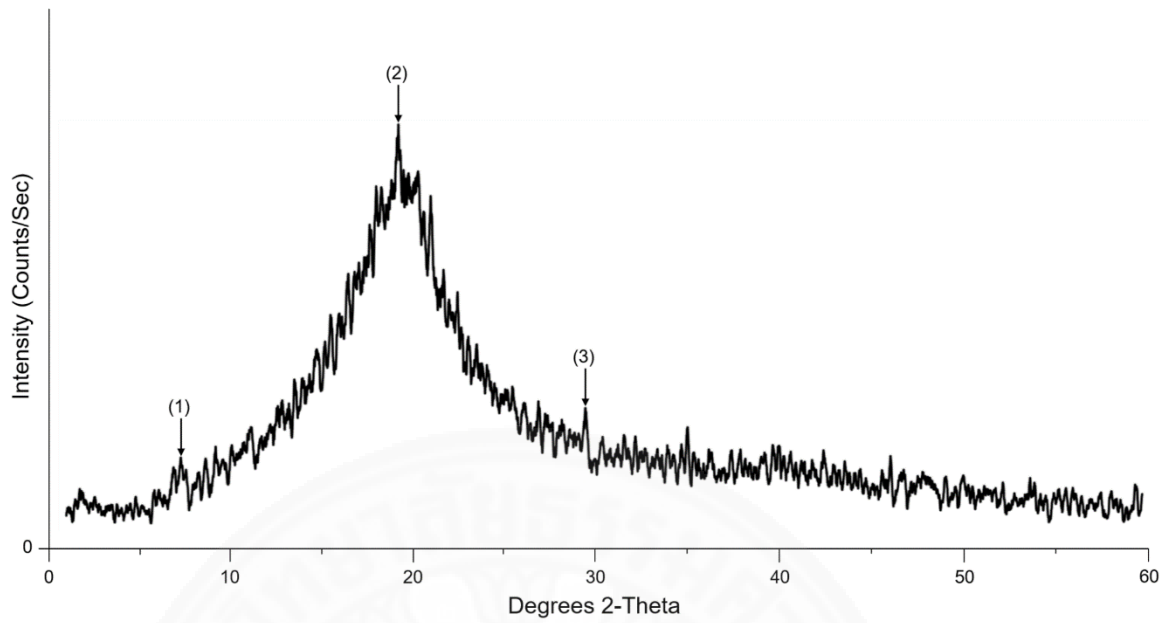| List	Degrees 2-Theta (°)	Intensity (Counts/sec)
1	11.70	14.62
2	13.00	16.20
3	16.58	14.63
4	18.69	31.03
5	20.64	43.62
6	21.97	13.06
7	25.06	47.17
8	38.27	21.57

Figure D2 X-ray powder diffraction pattern of phosphatidylcholine.

Table D2 Details of X-ray powder diffraction analysis of phosphatidylcholine.

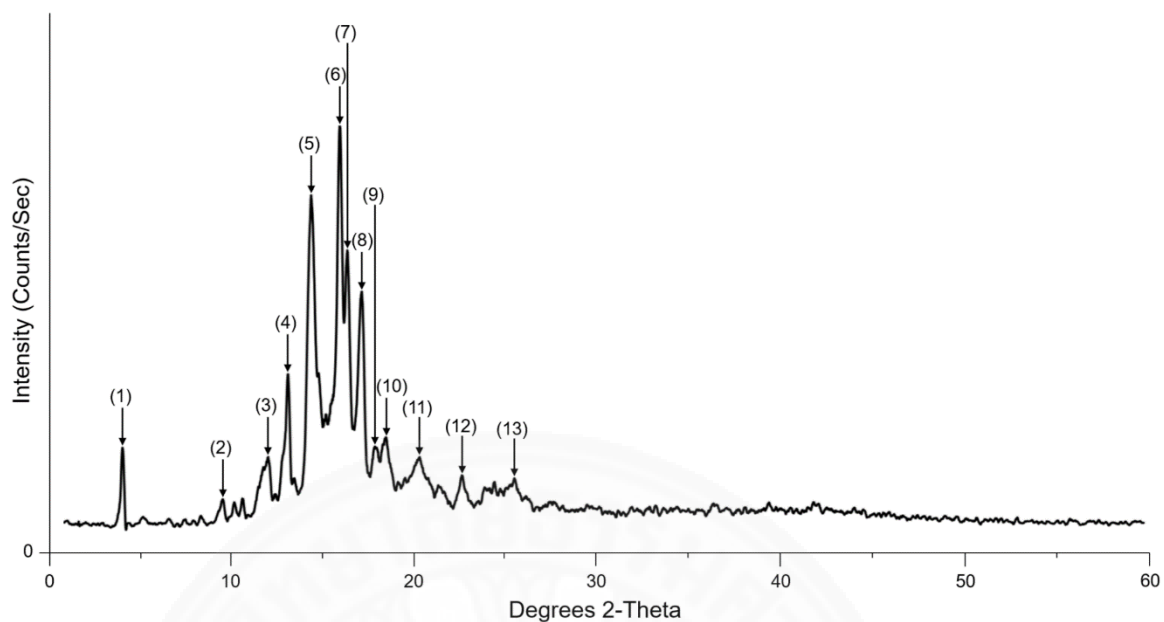| List	Degrees 2-Theta (°)	Intensity (Counts/sec)
1	8.19	5.77
2	19.90	27.39
3	30.01	8.94

Figure D3 X-ray powder diffraction pattern of cholesterol.

Table D3 Details of X-ray powder diffraction analysis of cholesterol.

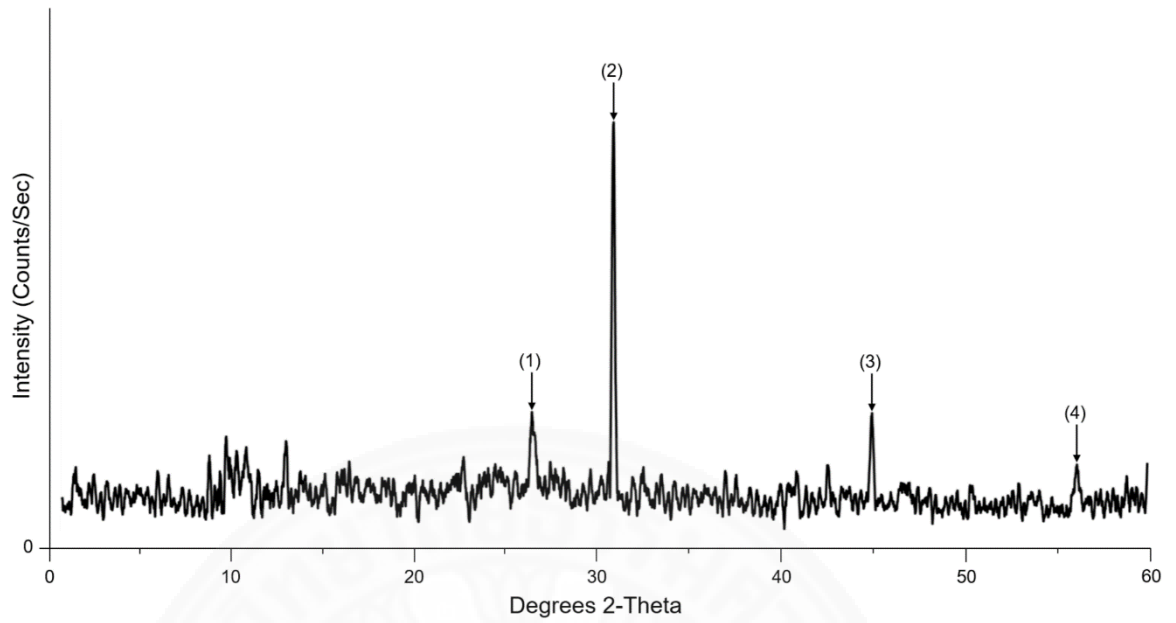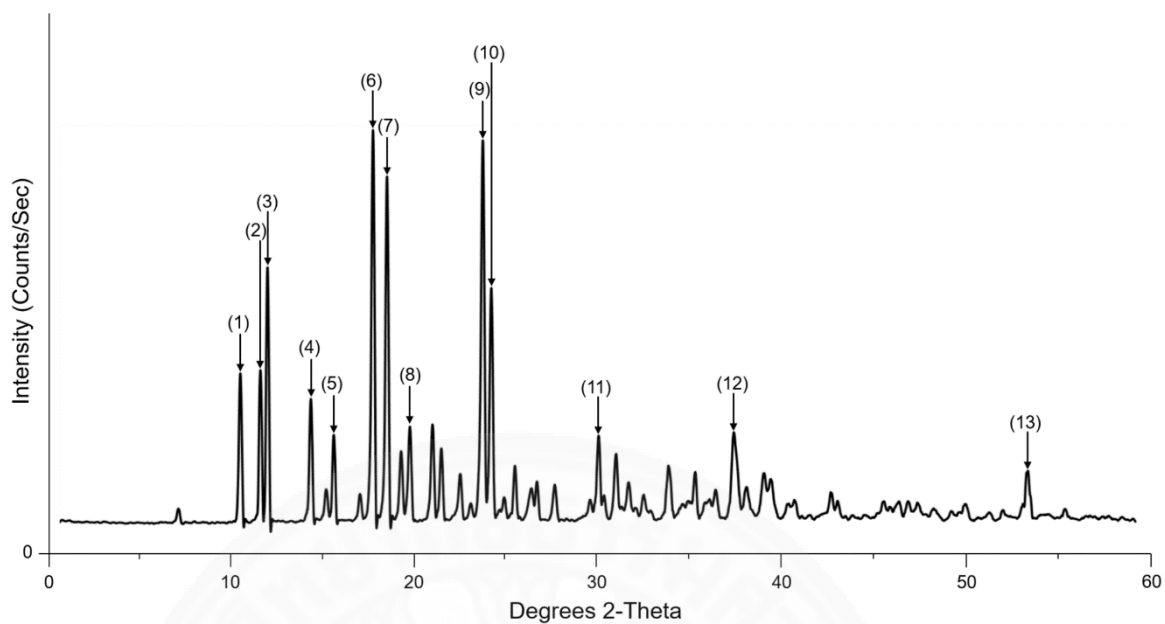| List	Degrees 2-Theta (°)	Intensity (Counts/sec)
1	5.16	31.93
2	10.52	12.24
3	13.04	27.92
4	14.08	61.24
5	15.30	131.02
6	16.83	158.07
7	17.23	109.19
8	18.04	92.91
9	18.72	33.04
10	19.35	36.65
11	21.10	29.06
12	23.47	20.46
13	26.20	20.85

Figure D4 X-ray powder diffraction pattern of SCP.

Table D4 Details of X-ray powder diffraction analysis of SCP.

List	Degrees 2-Theta (°)	Intensity (Counts/sec)
1	27.11	3.82
2	31.47	13.07
3	45.26	3.69
4	56.25	2.08

Figure D5 X-ray powder diffraction pattern of sucrose.

Table D5 Details of X-ray powder diffraction analysis of sucrose.

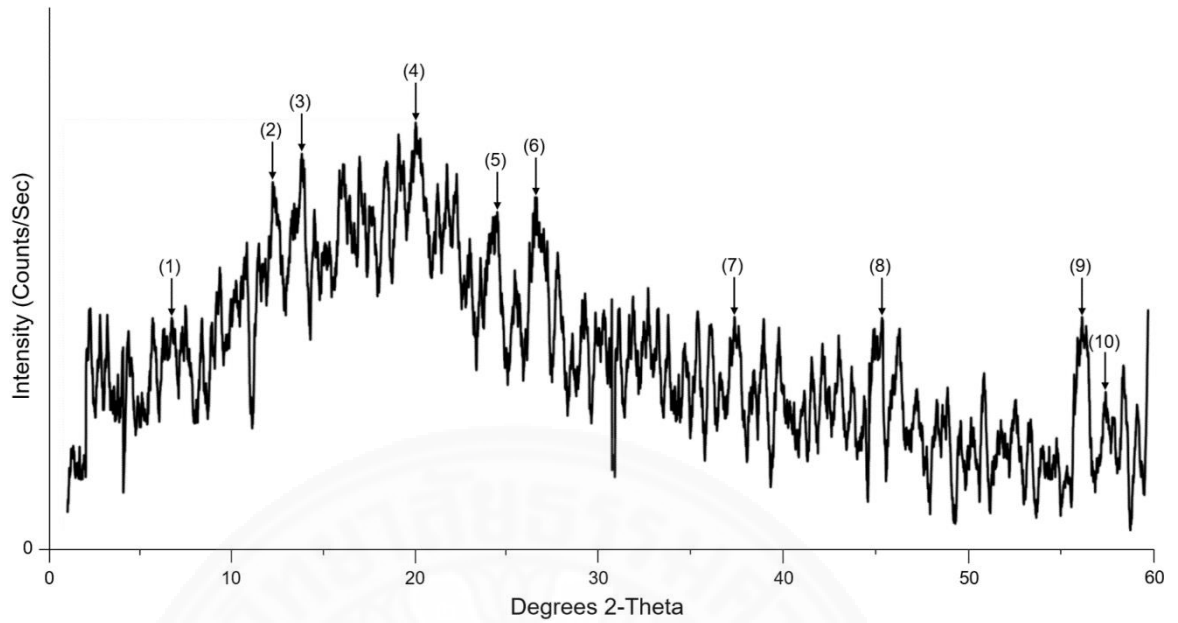| List	Degrees 2-Theta (°)	Intensity (Counts/sec)
1	11.74	127.69
2	12.82	131.43
3	13.20	219.27
4	15.54	107.21
5	16.74	75.02
6	18.89	336.43
7	19.64	299.46
8	20.89	81.78
9	24.79	327.59
10	25.27	202.69
11	31.06	75.34
12	38.38	76.37
13	54.12	44.19

Figure D6 X-ray powder diffraction pattern of LSCP-LPs.

Table D6 Details of X-ray powder diffraction analysis of LSCP-LPs.

List	Degrees 2-Theta (°)	Intensity (Counts/sec)
1	7.60	2.83
2	13.01	3.90
3	4.60	4.12
4	20.72	4.37
5	25.07	3.68
6	27.19	3.80
7	37.82	2.81
8	45.73	2.80
9	56.45	2.84
10	57.73	2.22

APPENDIX E

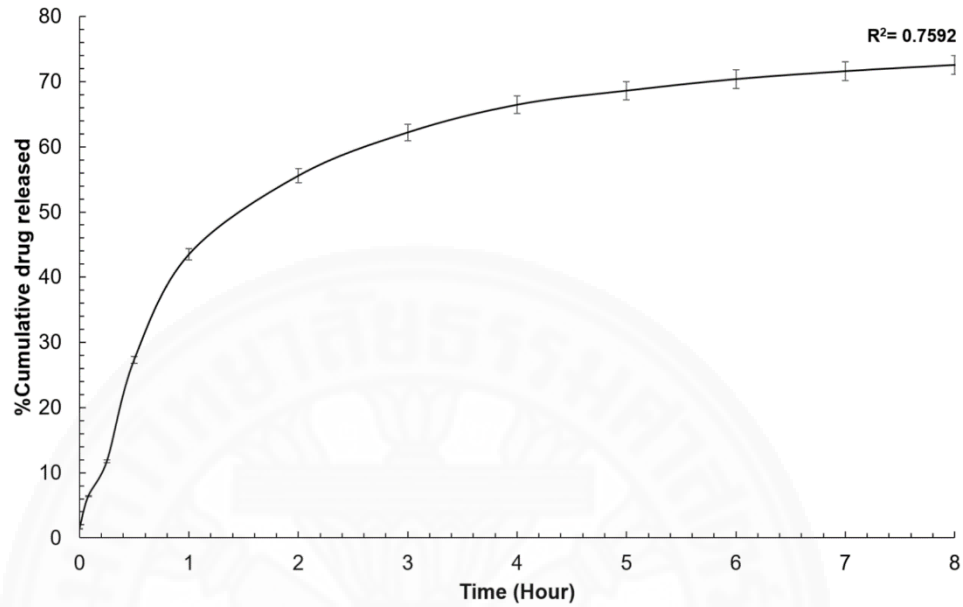## *IN VITRO* DRUG RELAESE PROFILES OF LSCP-LPs

Figure E1 Zero-order kinetic model of LSCP-LPs.

Table E1 Details of zero-order kinetic model of LSCP-LPs.

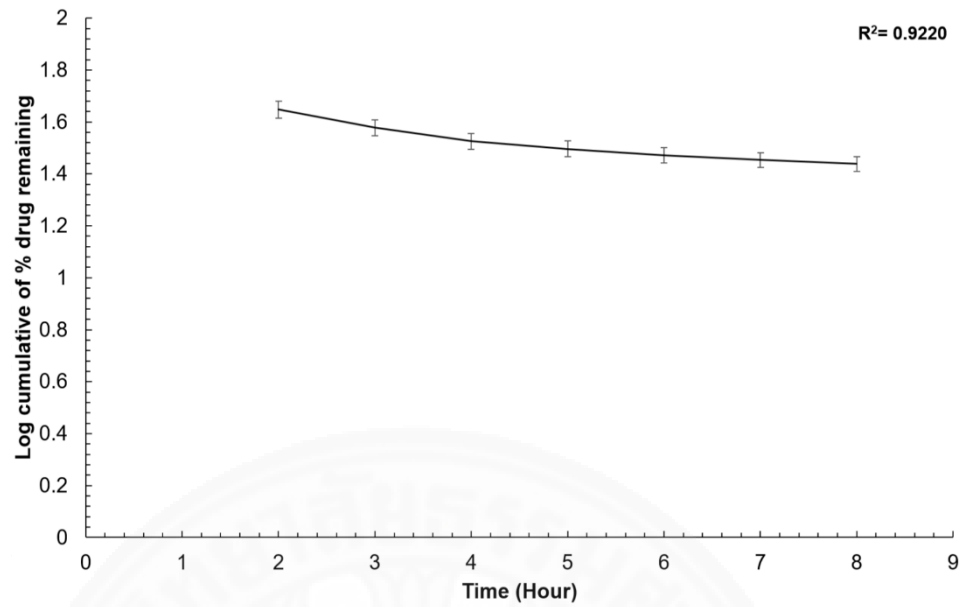| List	%Cumulative drug released	Time (Hour)
1	1.41±0.11	0.00
2	6.40±0.17	0.08
3	11.74±0.20	0.25
4	27.31±0.32	0.50
5	43.49±0.39	1.00
6	55.56±0.11	2.00
7	62.21±0.23	3.00
8	66.46±0.43	4.00
9	68.62±0.38	5.00
10	70.39±0.51	6.00

Figure E2 First-order kinetic model of LSCP-LPs.

Table E2 Details of first-order kinetic model of LSCP-LPs.

List	Log cumulative of % drug remaining	Time (Hour)
1	1.65±0.03	2.00
2	1.58±0.12	3.00
3	1.52±0.29	4.00
4	1.49±0.08	5.00
5	1.47±0.07	6.00
6	1.45±0.11	7.00
7	1.44±0.16	8.00
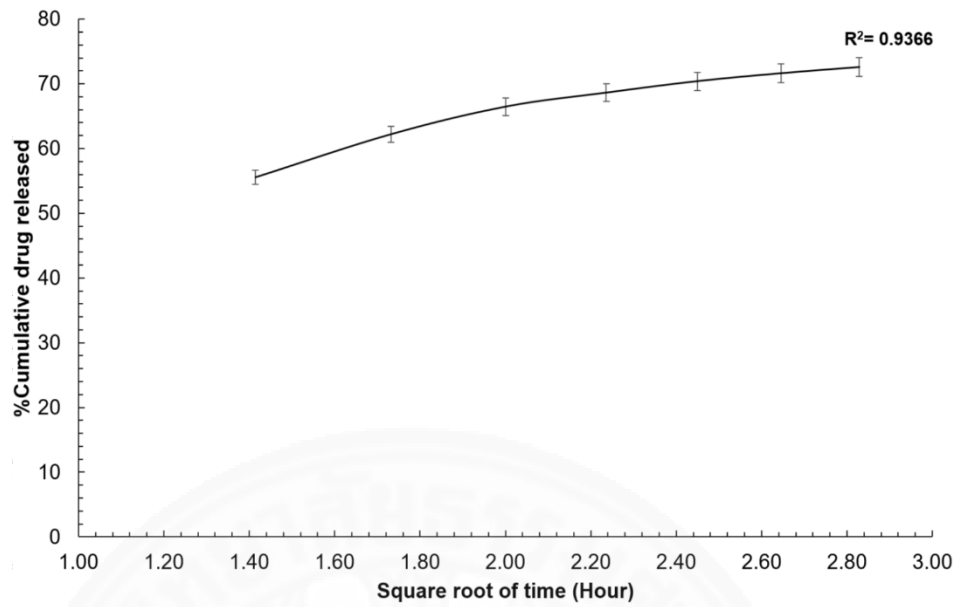
Figure E3 Higuchi's model of LSCP-LPs.

Table E3 Details of Higuchi's model of LSCP-LPs.

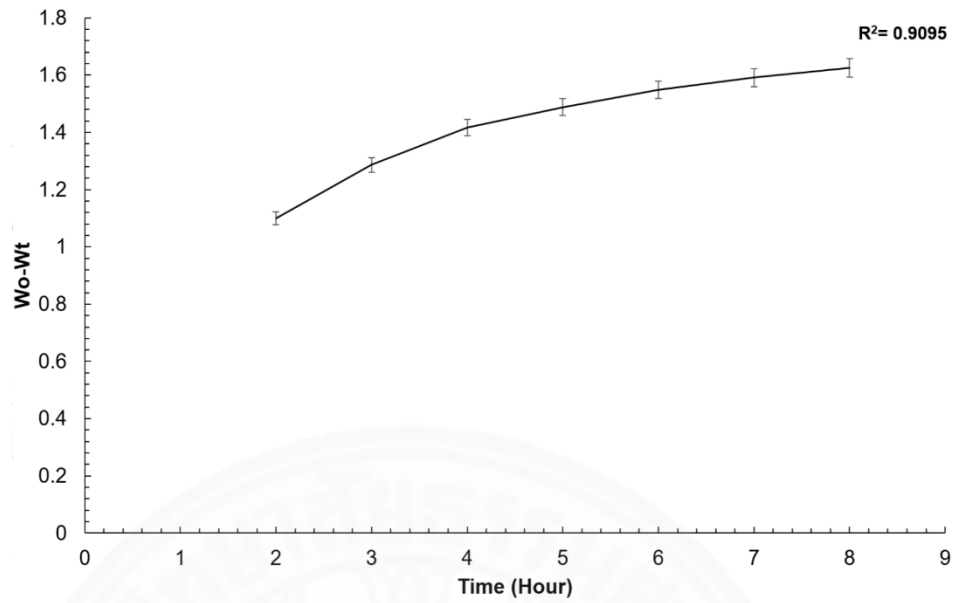| List	%Cumulative drug released	Square root of time (Hour)
1	55.56±0.11	1.41
2	62.21±0.23	1.73
3	66.46±0.43	2.00
4	68.62±0.38	2.24
5	70.39±0.51	2.45
6	71.61±0.36	2.65
7	72.56±0.44	2.83

Figure E4 Hixson-Crowell model of LSCP-LPs.

Table E4 Details of Hixson-Crowell model of LSCP-LPs.

List	W_o-W_t	Time (Hour)
1	1.10±0.07	2.00
2	1.29±0.11	3.00
3	1.42±0.03	4.00
4	1.49±0.20	5.00
5	1.55±0.14	6.00
6	1.59±0.09	7.00
7	1.63±0.18	8.00

BIOGRAPHY

Name	Mr. Tinnapop Touarawong
Date of Birth	April 17th, 1990
Educational Attainment	2008-2013: Bachelor of Pharmacy

Publications

Touarawong T, Rattanachuen W, Sarisuta N, Theerachayanan T, Samart C, Asasutjarit R. Preparation of lyophilized single chain polypeptide-loaded liposomes for ophthalmic use. Thai Journal of Pharmaceutical Sciences. 2017;41:97-100.

Outstanding award   June 27th, 2013: The Research Excellence Awards of Rangsit University in Title of Binding Efficiency Study of Flavonoids and Cyclooxygenase-2 by AutoDock 4.0 and AutoDock Vina 1.0 Programs from Rangsit University, Thailand.

November 2nd, 2012: The Silver Award of Poster Presentation in Title of "Binding Efficiency Study of Flavonoids and Cyclooxygenase-2 by AutoDock 4.0 and AutoDock Vina 1.0 Programs from The 1st International Conference on Herbal Medicines, Rangsit University, Thailand.